

OAK RIDGE NATIONAL LABORATORY  
Operated by  
UNION CARBIDE NUCLEAR COMPANY  
Division of Union Carbide Corporation



Post Office Box X  
Oak Ridge, Tennessee

ORNL  
NEPTON COPY  
~~CONFIDENTIAL~~

**ORNL**  
**CENTRAL FILES NUMBER**  
60-6-122

DATE: June 30, 1960  
SUBJECT: REVIEW OF INFORMATION ON U-MO ALLOYS  
AND U-MO-UO<sub>2</sub> DISPERSION FUELS  
TO: J. P. Hammond  
FROM: A. L. Lotts

COPY NO. 50

ABSTRACT

The status of development on U-Mo alloy and U-Mo-UO<sub>2</sub> dispersion fuels is reviewed. The physical and process metallurgy of these materials are given together with their chemical, thermal, and irradiation properties. A section is included on factors influencing the design of dispersion fuels.

~~CONFIDENTIAL~~  
~~CONFIDENTIAL~~  
~~CONFIDENTIAL~~  
~~CONFIDENTIAL~~  
~~CONFIDENTIAL~~

Full  
release  
David R. Hammond  
11/2/2011

## REVIEW OF INFORMATION ON U-MO ALLOYS AND U-MO-UO<sub>2</sub> DISPERSION FUELS

### I. INTRODUCTION

As a part of the program of the Oak Ridge National Laboratory for fast-breeder reactor fuels, the second phase is directed at the development of compartmented-ceramic- and dispersion-type fuels capable of operating at a temperature of 1250°F (676°C) or higher and for nuclear burnups in excess of 50 000 Mwd/ton. Moreover, these fuels must contain a large quantity of fertile material to obtain as high a breeding gain as possible during consumption of the fuel. As a part of Phase II, the advanced program, one of the objectives is to develop an element containing dispersed particles of UO<sub>2</sub> or possibly some other uranium compound made from highly enriched uranium in a matrix of a uranium-base alloy, made with depleted uranium. With such a fuel design, it may be possible to obtain a high burnup of the element as a whole without major damage to the matrix, while contributing to a high breeding gain. The present report contains a large portion of the information on U-Mo alloys and U-Mo-UO<sub>2</sub> cermetes that is available from the literature and from various installations.

### II. DISCUSSION OF AVAILABLE DATA AND TECHNOLOGY

The available data and information on the U-Mo system are quite generous for wrought material in the range of compositions up to 12 wt % Mo. However, the data are very sparse for alloy compositions containing greater than 12 wt % Mo. There is a very limited amount of information on the powder metallurgy of the U-Mo alloys and an even smaller amount on the U-Mo-UO<sub>2</sub> system. For example, Battelle Memorial Institute is the only laboratory in which a significant effort has been made to establish powder metallurgy techniques for fabricating the U-Mo-UO<sub>2</sub> fuel material; and all of their work was on UO<sub>2</sub> dispersed in the U-10 wt % Mo alloy and U-3.5 wt % Mo alloy.

Since the bulk of the information is on U-Mo alloys containing 12 wt % Mo, or less, it was apparent from the beginning of the survey that it would be necessary to extrapolate or deduce the behavior of the alloys containing higher than 12 wt % Mo. The alloy of primary interest is one containing 85 wt % U

and 15 wt % Mo. It is expected that this alloy will exhibit higher hot strength and better irradiation stability than the lower molybdenum alloys. Correspondingly, it is contemplated that the U-15 wt % Mo alloy will be more difficult to fabricate.

#### A. Physical Metallurgy of the U-Mo Systems

The phase equilibrium diagram for the uranium-rich portion of the U-Mo system is shown in Fig. 1, as reported by Rough and Bauer.<sup>1</sup> The diagram, as reported by Waldron *et al.*,<sup>2</sup> is shown in Fig. 2 and differs from the former in some respects, notably the gamma-to-delta (gamma-prime) transformation. (The notations gamma-prime and delta are used interchangeably, although gamma prime apparently is preferred because of current thinking that the gamma-prime phase is obtained through ordering of the gamma phase.)

##### 1. Crystal Structures

The alpha (high-uranium, low-temperature) phase has an orthorhombic crystal structure, and the gamma phase is body-centered cubic. Halteman<sup>3</sup> reports that the delta (gamma-prime) phase is of the  $\text{MoSi}_2$ -type (tetragonal) crystal structure and can be considered as an ordered form of gamma phase in which the molybdenum atoms assume special positions in a unit cell composed of three body-centered pseudocubes.

In early work on the U-Mo system, Pfeil and Browne<sup>4</sup> reported that the delta (gamma-prime) phase was a body-centered tetragonal structure with  $a = 3.425 \text{ \AA}$  and  $c = 3.282 \text{ \AA}$ , while Saller<sup>5</sup> and Halteman<sup>3</sup> had proposed a body-centered tetragonal phase with  $a = 6.84 \text{ \AA}$  and  $c = 6.55 \text{ \AA}$ . More recently, the delta (gamma-prime) phase was reported by Halteman<sup>3</sup> to be a tetragonal structure with  $a = 3.427 \text{ \AA}$  and  $c = 9.834 \text{ \AA}$ .

##### 2. Phase Equilibrium and Transformations

The reported equilibrium diagrams are shown in Figs. 1 and 2. The greatest interest is in the gamma to alpha plus delta (gamma-prime) transformation, since this transformation occurs in alloys of interest containing from approx 2 to 16 wt% Mo. The eutectoid composition of the binary system is approx 11.8 wt % Mo.

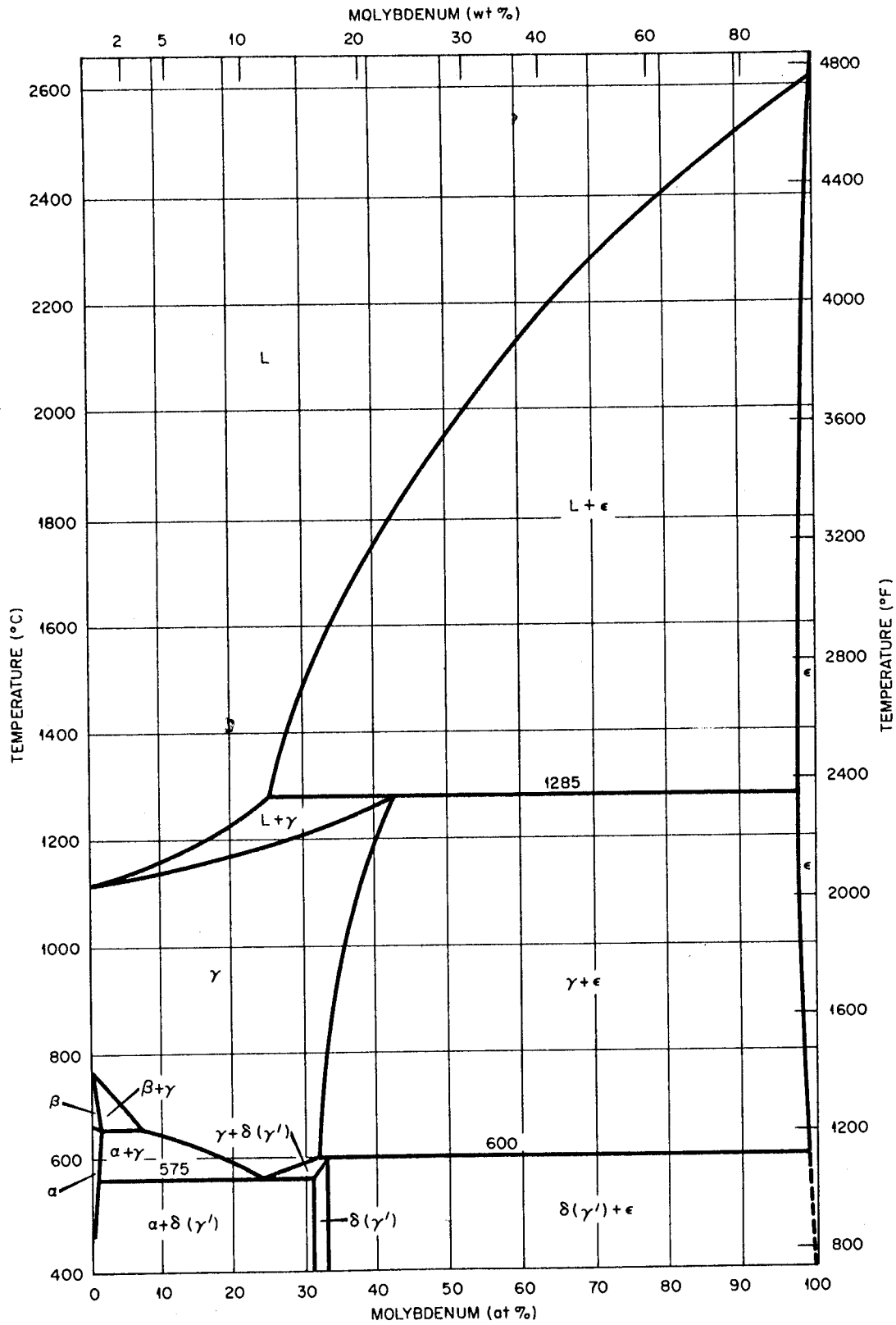


Fig. 1 Uranium-Molybdenum Constitution Diagram. Reference: F. A. Rough and A. A. Bauer, Constitution of Uranium and Thorium Alloys, BMI-1300, p. 41 (June 2, 1958).

UNCLASSIFIED  
ORNL-LR-DWG 47818

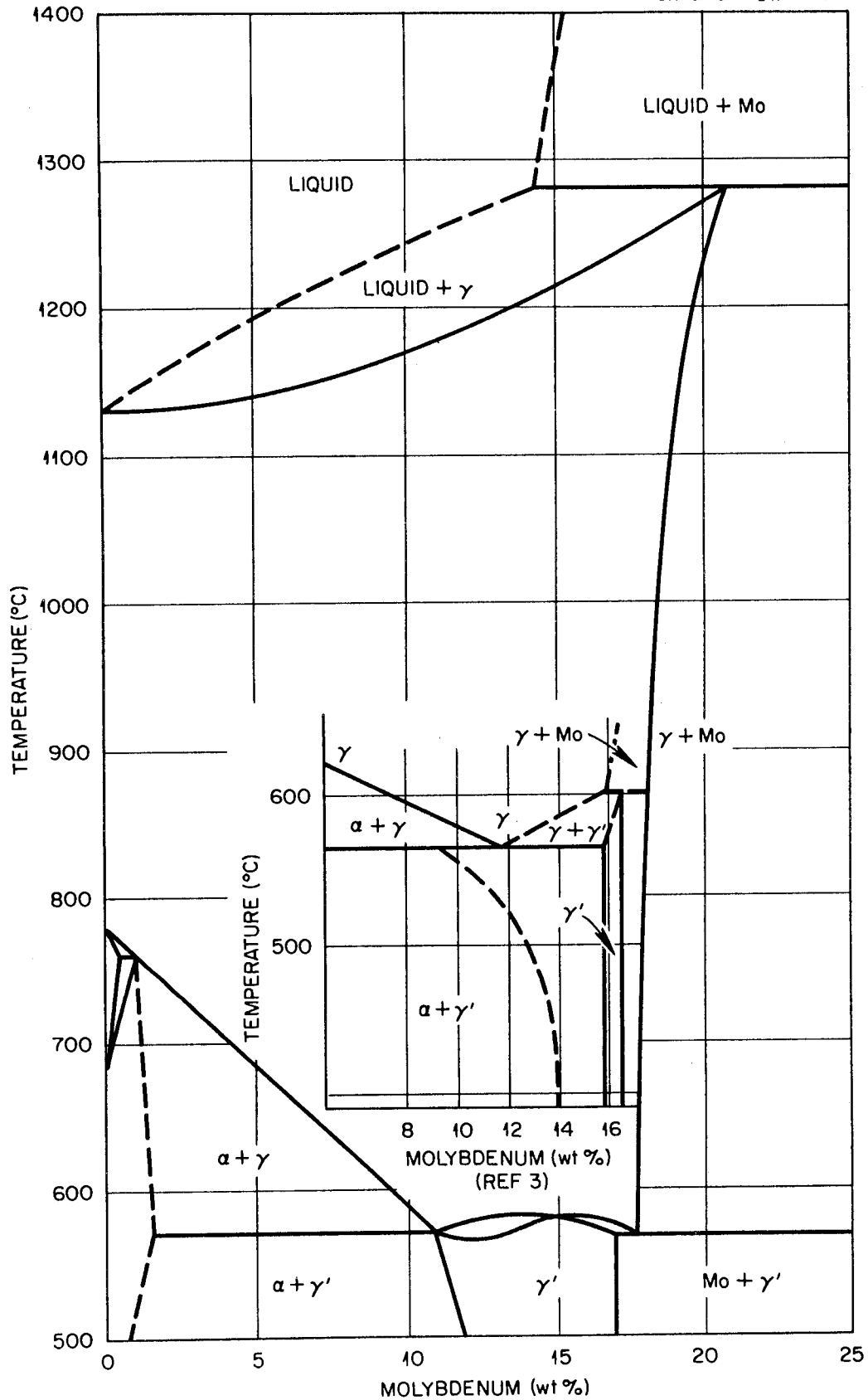


Fig. 2 Constitutional Diagram of the U-Mo System. Reference: M. B. Waldron, R. C. Burnett, and S. F. Pugh, The Mechanical Properties of Uranium-Molybdenum Alloys, AERE M/R 2554 (1958).

It has been shown that the decomposition of the gamma phase proceeds slowly in certain U-Mo alloys, thus enabling the retention of gamma phase at room temperature. The data show that the transformation becomes more sluggish as the molybdenum content of the gamma phase is increased. This is fortunate in that the prospect of having an isotropic alloy for use as a fuel material is enhanced. The advantages of such a material are obvious.

Studies have been conducted at various laboratories to ascertain the rates of transformation of the gamma phase. McGeary and Justusson<sup>6</sup> report the following changes in the structure of alloys after various heat treatments as indicated in Table I.

Table I. X-Ray Diffraction Identification of Phases in U-Mo Alloys After Various Heat Treatments

Alloy (wt%)	Heat Treatment	Phases Present
5.4 Mo	Quenched from 900°C	100% body-centered-cubic gamma, a = 3.477 A
5.4 Mo	Quenched from 900°C followed by 10-day anneal at 500°C	Approx 60% orthorhombic alpha Approx 40% body-centered-cubic gamma
5.4 Mo	Quenched from 900°C followed by 30-day anneal at 500°C	Approx 70% orthorhombic alpha Approx 30% Tetragonal gamma-prime
9.6 Mo	Quenched from 900°C	100% body-centered-cubic gamma, a = 3.413 A
9.6 Mo	Quenched from 900°C followed by 10-day anneal at 500°C	Approx 75% gamma Approx 20% alpha Approx 5% gamma-prime
9.6 Mo	Quenched from 900°C followed by 30-day anneal at 500°C	Approx 60% alpha Approx 40% gamma-prime
12.6 Mo	Quenched from 900°C	100% body-centered-cubic gamma, a = 3.413 A
12.6 Mo	Quenched from 900°C followed by 10-day anneal at 500°C	100% gamma
12.6 Mo	Quenched from 900°C followed by 30-day anneal at 500°C	20% alpha 80% gamma-prime
15.4 Mo	Quenched from 900°C	100% body-centered-cubic gamma, a = 3.395 A
15.4 Mo	Quenched from 900°C followed by 10-day anneal at 500°C	100% gamma
15.4 Mo	Quenched from 900°C followed by 30-day anneal at 500°C	100% gamma-prime (2 unidentifiable lines, neither alpha nor gamma)

It is notable that the U-15.4 wt % Mo alloy, some data for which are contained in Table I, is very close to the pure gamma-prime region.

Saller et al.<sup>7</sup> have studied the transformation kinetics of several U-Mo alloys by electrical-resistance measurement during isothermal transformation, supported by metallographic and hardness data. They concluded that transformation of the 21 at % (approx 10 wt %) molybdenum alloy occurs by a nucleation and growth mechanism, with the alpha and gamma-prime phases nucleating at the gamma grain boundaries and growing inwardly to consume the gamma grains. The decomposition products have a lamellar distribution. They state further that the 26.4 and 30 at % (approx 13 and 15 wt %) molybdenum alloys transform by an ordering reaction, which probably occurs by a nucleation and growth mechanism. Enough data were obtained in their investigation to indicate that the transformation of the 30 at % (15 wt %) Mo alloy had a "C-curve-type" behavior. Moreover, they concluded that the optimum temperature for transformation is about 500°C. Curves for the beginning of transformation of gamma at various temperatures for a series of U-Mo alloys ranging from 7 to 12 wt % Mo have been reported by McGeary et al.,<sup>8</sup> and these curves are shown in Fig. 3. The curves show that within the range of compositions investigated the transformation of gamma to alpha and gamma-prime becomes more sluggish as the molybdenum content is increased. The curves substantiate the conclusion of Saller et al. in that the noses of the curves fall near 500°C. Whether the nose of the U-15 wt % Mo curve would be further to the right than for the 12 wt % Mo alloy curve is not revealed in the literature. Intuitively, it would appear that the 15 wt % Mo alloy would show greater sluggishness to transformation than lower molybdenum alloys.

#### B. Properties of U-Mo Alloys

Subsequently discussed are the mechanical, physical, and irradiation properties of U-Mo alloys as reported in the literature.

##### 1. Physical Properties

The physical properties of U-Mo alloys ranging in composition from 9-15 wt % Mo have been reported by McGeary et al.<sup>8</sup> A summary of these properties is given in Table II and is for gamma phase (9-15 wt % Mo) alloys unless otherwise indicated.

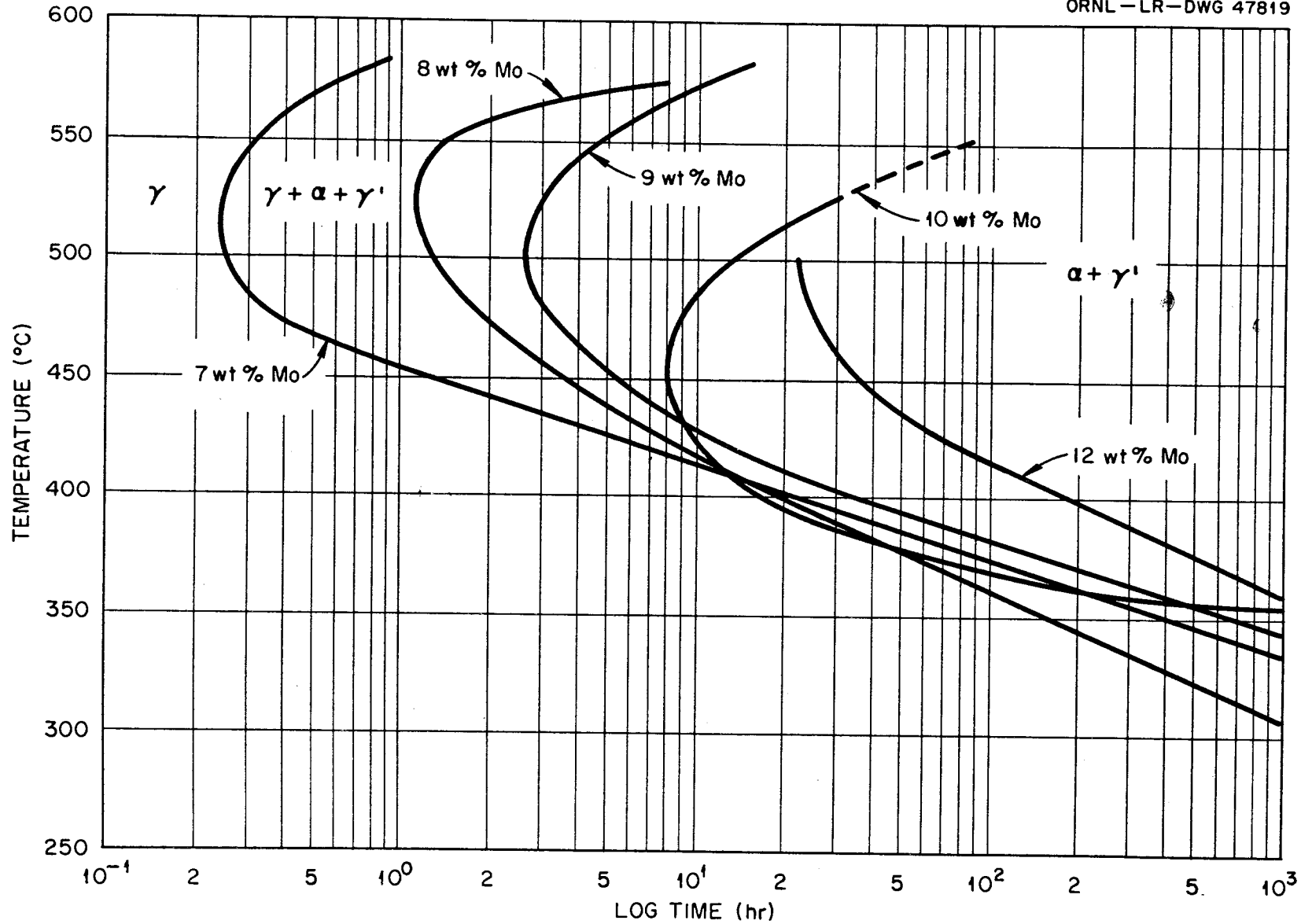


Fig. 3 Times for Beginning of Transformation as Affected by Molybdenum Content. Reference: R. K. McGearry *et al.*, Development and Properties of Uranium-Base Alloys Corrosion Resistance in High Temperature Water-Part I, WAPD-127 (April 25, 1955).

Table II. Physical Properties of Uranium-Molybdenum Alloys

Property	Alloy	Measurement
Thermal Conductivity (10-100°C)	U-8 wt % Mo	0.034 cal/(sec-cm <sup>2</sup> -°C/cm)
	U-12 wt % Mo	0.033 cal/(sec-cm <sup>2</sup> -°C/cm)
Thermal Coefficient of Expansion (100-400°C)	U-8 wt % Mo	13.8 0.5 x 10 <sup>-6</sup> /°C
	U-12 wt % Mo	13.0 0.5 x 10 <sup>-6</sup> /°C
Specific Heat (300-400°C)	U-12 wt % Mo	7-8 cal/mole/°C
Electrical Resistivity	Gamma Phase	73 μohm cm at 25°C
	(9-15 wt % Mo)	65 μohm after 42 days at 400°C
Density	U-8 wt % Mo	17.5 g/cc
	U-12 wt % Mo	16.9 g/cc
Recrystallization	Gamma Phase	1 hr at 600°C for 75%
	(9-15 wt % Mo)	reduction

Thermal expansion. The thermal dilation curves of U-Mo alloys is given in Fig. 4, as reported by McGearry et al.<sup>8</sup> It is notable that the 15 wt % Mo alloy tested after 16 days annealing at 550°C shows excellent thermal stability. The linear thermal expansions of U-Mo alloys are given in Fig. 5.

Density. The variation of density of U-Mo alloys quenched from 900°C with the molybdenum composition is given in Fig. 6. Del Grosso<sup>9</sup> reports that the density of the 10 wt % Mo alloy at room temperature is 17.1 g/cc for the metastable gamma phase, while the fully transformed structure has a density of 17.3 g/cc.

UNCLASSIFIED  
ORNL-LR-DWG 47820

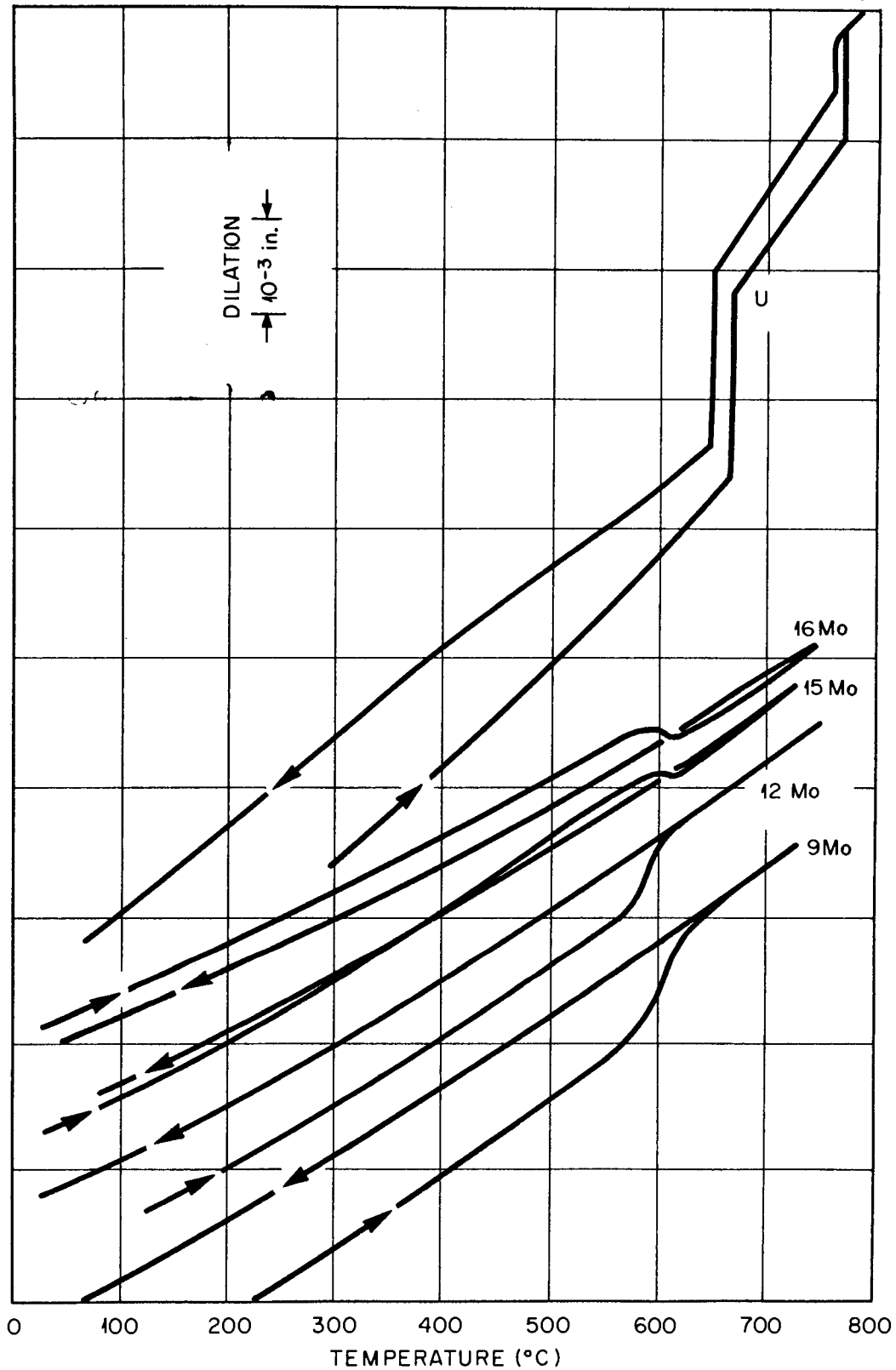


Fig. 4 Thermal Dilation of Natural U and U-Mo Alloys after Annealing at 550°C for 16 Days. Reference: R. K. McGearry *et al.*, Development and Properties of Uranium-Base Alloys Corrosion Resistance in High Temperature Water-Part I, WAPD-127 (April 25, 1955).

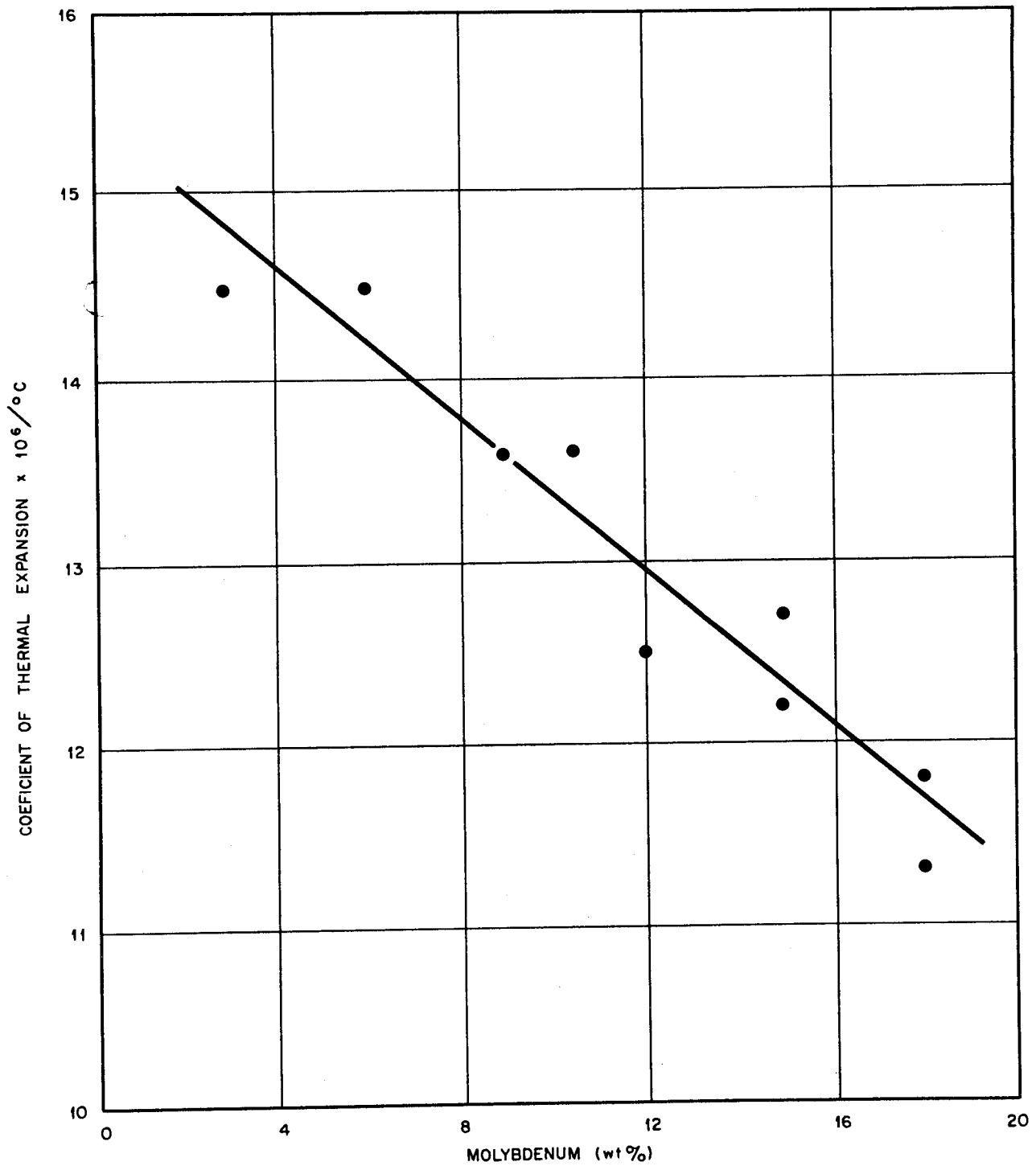


Fig. 5 Linear Thermal Expansivity for U-Mo Alloys in the Temperature Range 100-400°C. Reference: R. K. McGeary et al., Development and Properties of Uranium-Base Alloys Corrosion Resistance in High Temperature Water-Part I, WAPD-127 (April 25, 1955).

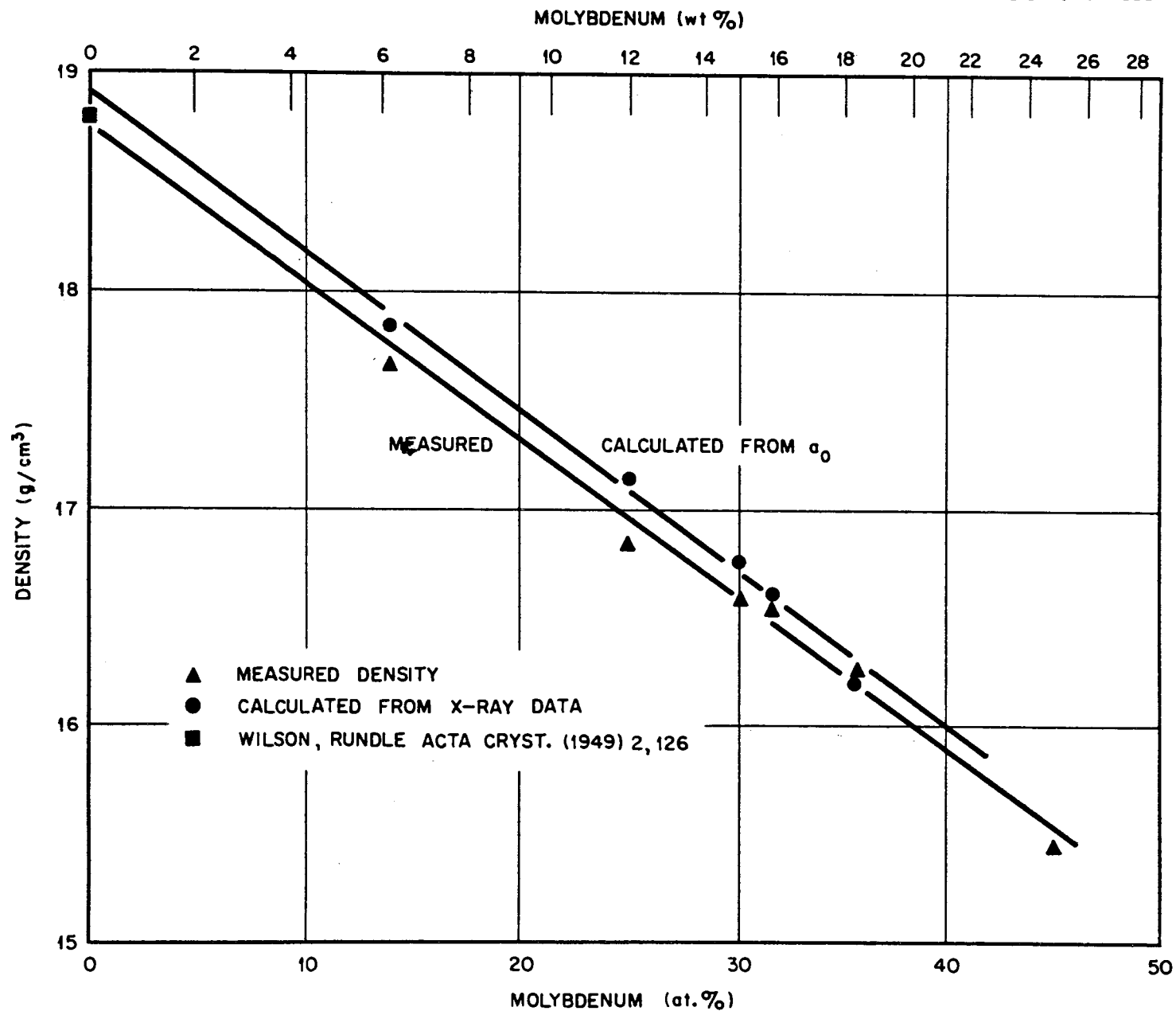


Fig. 6 Density of U-Mo Alloys Quenched from 900°C. Reference: R. K. McGeary *et al.*, Development and Properties of Uranium-Base Alloys Corrosion Resistance in High Temperature Water-Part I, WAPD-127 (April 25, 1955).

## 2. Mechanical Properties

The mechanical properties of U-Mo alloys have been determined by various laboratories, but data on the 15 wt % Mo alloy are lacking. Gates et al.<sup>10</sup> have obtained tensile data for the 10 wt % Mo alloy given in Table III. They have also determined the elastic modulus and yield strength, which are given in Table IV, for this alloy from bend-test data.

Waldron<sup>2</sup> and his co-workers have determined the hardness and tensile properties of a series of U-Mo alloys after being heat treated in various manners. The alloys containing 0.85-7.5 wt % Mo were fabricated by casting, forging, and hot rolling. Alloys containing 10-13.5 wt % Mo were cast as 1-in.-diam bars and were tested in this structural condition because of their tendency to crack during hot working. In melting these alloys, excessive carbon could have been picked up because of the use of unwashed graphite crucibles and molds, thus embrittling the final cast material. A separate batch of 10.9 wt % Mo alloy specimens were produced by extrusion. The detailed procedures used in fabricating these alloys are given in a subsequent section of this report (see p. 39). All samples were first homogenized at 900°C and water quenched; and, after each subsequent heat treatment, they were water quenched. The gamma phase was retained upon quenching in alloys containing greater than 6.6 wt % Mo, but it partially or completely decomposed in alloys with less molybdenum.

The structures obtained by various heat treatments of the alloys are given in Table V. The mechanical properties of part of these alloys at room temperature are given in Table VI, and hot-hardness data are given in Table VII. Table VIII contains data on the mechanical properties of these alloys at elevated temperatures. More detailed analysis of the properties of the 10.9 wt % Mo alloy is afforded by Table IX, which gives the ultimate tensile strength, elongation, and hardness after various heat treatments of this alloy, clad and unclad with zirconium. Observe that the specimens heat treated at 550°C show a significant reduction in ductility indicating that transformation of the gamma phase had begun. The data in Table VII show that the hot hardness of the gamma phase increases as the molybdenum content of the alloy is increased, at least up to 13.5 wt %. High-hot-hardness values were obtained where the gamma phase had started to decompose.

TABLE III. Tensile Strength of Unirradiated U-10 wt % Mo Alloy<sup>a</sup>

Specimen No.	Test Temp. °C	Elastic Mod. 10 <sup>6</sup> psi	0.2% Offset Y.S. psi	Ultimate T.S. psi	Elongation %	Reduction in Area, %
1	25	12.8	138 600	141 800	1.5 in 2 in.	33.8
2	25	12.2	136 400	139 000	1.9 in 2 in.	36.8
(Average)	25	12.5	137 500	140 400	1.7 in 2 in.	35.3
1	250	12.3	86 300	91 600	10.5 in 1 in.	45.2
2	250	11.8	85 200	90 800	4.5 in 2 in.	45.7
(Average)	250	12.0	85 800	91 200		45.4
1 <sup>b</sup>	500	9.4	66 200	69 400	1.5 in 1 in.	15.1

<sup>a</sup>J. E. Gates, E. G. Bodine, J. C. Bell, A. A. Bauer, and G. D. Calkins, Stress-Strain Properties of Irradiated Uranium-10 wt % Molybdenum, BMI-APDA-638, (Jan. 6, 1958).

<sup>b</sup>Two others at 500°C were scheduled. They were not straight, however, and broke when straightened by the grips.

TABLE IV. Mechanical Properties of Unirradiated U-10 wt % Mo Alloy Determined from Bend-Test Data<sup>a</sup>

Specimen No.	Test Temp. °C	Elastic Modulus 10 <sup>6</sup> psi	0.2 Offset Y.S. psi <sup>b</sup>
1	25	12.5	
2	25	12.5	
(Average)	25	12.5	
1	250	11.4	75 600
2	250	12.1	
3	250	12.3	86 600
(Average)	250	11.9	81 100
1	500	8.1	64 000
2	500	8.4	
3	500	9.8	
4	500	9.8	78 500
(Average)	500	9.0	71 200

<sup>a</sup>J. E. Gates, E. G. Bodine, J. C. Bell, A. A. Bauer, and G. D. Calkins, Stress-Strain Properties of Irradiated Uranium-10 wt % Molybdenum, BMI-APDA-638, (Jan. 6, 1958).

<sup>b</sup>Where values are not shown, the test was stopped before plastic straining took place.

TABLE V. Structures of U-Mo Alloys Obtained  
by Various Heat Treatments<sup>a</sup>

Composition wt % Mo	Heat Treatment		Structure	
	Temp. °C	Time (days)		
0.85, 1.5, 2.2	400	1	$\gamma$ decomposed to $\alpha + \gamma$ or $\gamma'$	
	400	7		
	400	21		
	500	1		
	500	7		
	500	21		
	600	(8 hours)		$\alpha +$ retained $\gamma$
	600	2		
	600	7		
	650	14		$\alpha + \gamma$ (partially decomp. on quenching)
2.2, 4.6, 6.6	585	21	$\alpha +$ retained $\gamma$	
4.6, 6.6, 7.8, 10.0	450	14	$\alpha + \gamma'$	
10.9	575	28	$\gamma + \gamma'$ (almost complete to $\gamma'$ ) <sup>b</sup>	
10.9, 13.5	550	28	$\gamma'$	

<sup>a</sup>M. B. Waldron, R. C. Burnett, and S. F. Pugh, The Mechanical Properties of Uranium-Molybdenum Alloys, AERE M/R 2554 (1958).

<sup>b</sup>There appears to be no difference in mechanical properties of materials containing essentially gamma-prime from that of the disordered quenched gamma phase.

TABLE VI. Mechanical Properties of U-Mo Alloys at Room Temperature<sup>a</sup>

Nominal Composition wt % Mo <sup>b</sup>	Heat Treatment		Hardness V.D.P. (avg)	Ultimate Tensile Strength psi	Elong. (on 1.2 in.) %	Young's Mod. 10 <sup>6</sup> psi	Rigidity Mod. 10 <sup>6</sup> psi	Poisson's Ratio
	Temp. °C	Time (days)						
Uranium Unalloyed	Cast and Annealed		187	70 000	5	26		
4.6	900	7	377	138 800	2.5	14.6	5.3	0.36
	585	21	423	125 600	1.6	(21.5)	(8.2)	(0.30)
							(14.4)	(5.5)
	450	14	482	97 400	1.6	22.4	8.6	0.29
6.6	900	7	255	113 200	8.2	11.4	4.0	0.39
	585	21	(336)	(144 200)	(6.5)	(20.3)	(8.0)	(0.28)
				(365)	(133 000)	(1.6)	(14.6)	(5.4)
	450	14	616	131 600	0.6	21.3	8.4	0.30
7.8	900	7	288	94 000	1.2	11.4	4.1	0.37
	450	14	500	38 800	2.5	18.9	7.3	0.30
10.0	900	7	311	89 600	0.1	12.6	4.7	0.35
	450	14	541	42 600	0.8	17.3		0.33
10.9	900	7	331	89 000	1.4	13.6	5.9	0.35
	575	28	319	65 400	0.6	14.0	5.2	0.35
13.5	900	7	374	47 000	nil	13.4	4.9	0.35

<sup>a</sup>M. B. Waldron, R. C. Burnett, and S. F. Pugh, The Mechanical Properties of Uranium-Molybdenum Alloys, AERE M/R 2554 (1958).

<sup>b</sup>Similar data on 1.5 and 2.2 wt % Mo alloys are contained in the referenced report.

TABLE VII. Hot-Hardness Values for U-Mo Alloys\*

Alloy and Prior Heat Treatment	Test Temp. °C	Hot Hardness V.P.H.	Alloy and Prior Heat Treatment	Test Temp. °C	Hot Hardness V.P.H.	Alloy and Prior Heat Treatment	Test Temp. °C	Hot Hardness V.P.H.	Alloy and Prior Heat Treatment	Test Temp. °C	Hot Hardness V.P.H.
7.8 wt % Mo	20	297	10.0 wt % Mo (cast)	20	316	10.9 wt % Mo	20	348	13.5 wt % Mo	20	300
900°C, 7 days	100	266	900°C, 7 days	100	277	900°C, 7 days	100	254	900°C, 7 days	100	290
	200	166		200	237		200	245		200	321
	300	122		300	200		300	147		300	254
	400	124		400	183		400	130		400	234
	500	113		500	132		500	117		500	219
	600	73.6		600	128		600	99.8		600	153
	700	27.7		700	78.5		700	81.6		700	86.3
	800	29.2		800	50		800	44.3		800	55.8
900°C, 7 days	20	520	900°C, 7 days	20	541	900°C, 7 days	20	352			
	100	366		100	446		100	118			
	200	304		200	216		200	68.8			
450°C, 14 days	300	206	450°C, 14 days	300	138	550°C, 28 days	300	64			
	400	139		400	74.2		400	80.7			
						900°C, 7 days	500	47.7			
							20	323			
							100	274			
							200	271			
							300	251			
							400	934			
						500	64.6				

\* M. B. Waldron, R. C. Burnett, and S. F. Pugh, The Mechanical Properties of Uranium-Molybdenum Alloys, AERE M/R 2554 (1958).

TABLE VIII. Mechanical Properties of U-Mo Alloys at Elevated Temperature\*

Nominal Composition wt % Mo	Prior Heat Treatment		Ultimate Tensile Strength		Young's Mod. 10 <sup>6</sup> psi	Elongation (on 1.2 in.) %
	Temp. °C	Time (days)	Temp. °C	psi		
7.8	900	7	200	76 800	11.4	6
			400	71 200	10.2	9
			600	50 000	11	5
			800	8 200	5.4	69
10.0	900	7	200	74 000	10.7	0.5
			400	52 000	7.5	1
			600	26 000	4.8	0
			800	8 000	6.0	3.0
	450	14	200	44 000	13.3	nil
			300	26 600	15.0	0.5
			400	37 200	15.8	0.5
10.9	900	7	400	51 000	11	0.5
			600	18 800	8.8	0.5
			700	21 200	8.0	1
			800	21 200	7.4	6
10.0	575	28	400	21 600	12.2	2
			600	18 000	8.6	0.5
			800	12 600	8.6	11

\*M. B. Waldron, R. C. Burnett, and S. F. Pugh, The Mechanical Properties of Uranium-Molybdenum Alloys, AERE M/R 2554 (1958).

TABLE IX. The Mechanical Properties of U-10.9 wt % Mo Alloy after Heat Treatment\*

Annealing Temperature °C	Time (days)	Annealing Environment	Room Temperature Properties		
			U.T.S. psi	Elong. %	Hardness V.P.H.
(a) Not annealed			155 400	7.5	347
(b) 45	2	In bonded co-extruded Zircaloy sheath in loose stainless steel can	191 000	1.	423
(c) 65	2	As for (b)	151 200	9.0	353
(d) 800	2	As for (b)	144 000	6.	356
(e) 650	2	In bonded co-extruded Zircaloy sheath	151 400	6.	331
(f) 650	2	Bare	152 000	5.0	346
(g) 650	2	Bare canned in stainless steel	150 000	5.0	344
(h) 550	2	As for (e)	148 000	1.6	350
(i) 550	1 hour	As for (e)	148 000	0.6	353
(j) 650	2 hours	Bare in air	73 000	nil	336

\* M. B. Waldron, R. C. Burnett, and S. F. Pugh, The Mechanical Properties of Uranium-Molybdenum Alloys, AERE M/R 2554 (1958).

Saller et al.<sup>11</sup> have also determined the hot hardness of U-Mo alloys. Their alloys were induction melted in a vacuum and poured from zirconia crucibles into cold graphite molds. The ingots were subsequently melted by the consumable electrode arc-melting process, after which the ingots so produced were machined and reduced by forging, rolling, and swaging to rods approx 7/8 in. in diameter. The fabrication history and the heat treatments of the alloys are given in Table X. The hardness data that they collected on 7- 9- and 12-wt % Mo alloys are contained in Table XI. McGearry et al.<sup>8</sup> report a hardness value of 300 DPH for the U-12 wt % Mo, which corresponds favorably with the above data.

### 3. Irradiation Behavior

The U-10 wt % Mo alloy has been irradiated rather extensively, and enough information is available to give an indication of the irradiation behavior of this alloy. With other U-Mo alloys, the situation is not so fortunate.

Fawcett<sup>12</sup> reports that bare 10 wt % Mo specimens show density changes of about 2.5%/at.% burnup. Zirconium-clad coextruded specimens have split at the ends when irradiated to burnups between 2.0 and 2.7 at.%. In the Battelle Memorial Institute work, volume changes of 2.1-7.4%/total at.% burnup were observed on the specimens that split. Their data on a series of clad specimens are given in Table XII. In addition to the above data, clad coextruded 9- and 12-wt % Mo alloys have been irradiated to burnups of 3.12 and 3.04 at.% with density decreases on the order of 3.5%/total at.% burnup.

Bend-test data on U-Mo alloys, reported by Gates et al.<sup>10</sup> are given in Table XIII. Conclusions drawn from these data were:

1. The instability of the gamma phase during mechanical testing in the vicinity of 500°C affects the physical properties of the reference alloy (U-10 wt % Mo) both in the unirradiated and irradiated condition.

TABLE X. Fabrication and Heat Treating Temperatures  
for BMI U-Mo Alloys\*

Nominal Composition wt % Mo	Forging Temperature, °F	Rolling Temperature, °F
3.5	1125 (607°C)	1125 (607°C)
5.0	1500 (816°C)	1500 (816°C)
7.0	1600 (871°C)	1600 (871°C)
9.0	1800 (982°C)	1650 (899°C)
12.0	1800 (982°C)	1800 (982°C)

Heat Treatments:

- G: 1 hr at 800°C, water quenched gamma, used on all compositions
- L: 1 hr at 800°C, furnace cooled to 500°C, held 200 hr, furnace cooled, used on 9 wt % Mo
- M: 1 hr at 800°C, furnace cooled to 500°C, held 2 weeks, furnace cooled, used on 12 wt % Mo
- K: Same as M except 100 hr at 500°C, used on 7 wt % Mo

---

\* J. E. Gates, E. G. Bodine, J. C. Bell, A. A. Bauer, and G. D. Calkins, Stress-Strain Properties of Irradiated Uranium-10 wt % Molybdenum, BMI-APDA-638, (Jan. 6, 1958).

TABLE XI. Hot Hardness of U-Mo Alloys<sup>a</sup>

Mo Content wt %	Heat Treatment <sup>b</sup>	Hardness DPH, kg per mm <sup>2</sup>							
		Room Temperature	600°C	650°C	680°C	700°C	725°C	750°C	800°C
7.0	G	248	34	35		24		17.4	14.8
7.0	K	448	47.2	38.1	34.0	31.4	23.9	20.6	13.3
9.0	G	276	89	69		51		38	30
9.0	L	423	86.9	78.3	65.3	58.2	48.3	41.1	27.7
12.0	G	310	122	92		72		49	37.0
12.0	M	312	158	112	105	93	78.8	67.4	47.4

<sup>a</sup>J. E. Gates, E. G. Bodine, J. C. Bell, A. A. Bauer, and G. D. Calkins, Stress-Strain Properties of Irradiated Uranium-10 wt % Molybdenum, BMI-APDA-638, (Jan. 6, 1958).

<sup>b</sup>Heat Treatments:

G: 1 hr at 800°C, water quenched gamma, used on all compositions

L: 1 hr at 800°C, furnace cooled to 500°C, held 200 hr, furnace cooled, used on 9 wt % Mo

M: 1 hr at 800°C, furnace cooled to 500°C, held 2 weeks, furnace cooled, used on 12 wt % Mo

K: Same as M except 100 hr at 500°C, used on 7 wt % Mo

TABLE XII. Results of the Irradiation of U-Mo Alloys, Cladding-Thickness Series<sup>a</sup>

Specimen <sup>b</sup>	Capsule	Burnup <sup>c</sup> Total at. %	Calculated <sup>d</sup> Av Centered Core Temp. °C	Dimensional Data Percent Change				Density Decrease per Total Burnup, at. %	Comments on Macroscopic Condition
				Diameter Increase	Length Increase	Volume Increase	Density Decrease		
1OCT-4-26	9-9B	2.7	385	9.5	5.1	26.0	17.3	6.4	Crack at one end
1OCT-8-3	9-9B	2.1	385	7.9	6.8	24.3	15.1	7.2	Good condition
1OCT-11-3	9-9B	2.4	385	5.7	6.9	13.2	9.7	4.2	One end split
1OCT-4-25	9-9A	2.1	340	8.3	4.8	22.9	15.5	7.2	Good condition
1OCT-8-2	9-9A	2.1	340	3.9	2.1	10.2	8.2	3.9	One end split
1OCT-11-2	9-9A	2.0	340	2.3	0.4 <sup>e</sup>	5.1	4.2	2.1	Both ends split

<sup>a</sup>S. L. Fawcett, A Study of Core Fuel Systems for a Fast Breeder Power Reactor, BMI-APDA-636, November 5, 1957.

<sup>b</sup>The specimens were arranged top to bottom according to their position in capsules. Specimens 4, 8, and 11 identify cladding thicknesses of 4.7, 8.1, and 11 mils, respectively. Specimens were co-extruded and heat treated 1 hr at 800°C, quenched, and held 15 min at 350°C.

<sup>c</sup>Burnups calculated from dosimeter data.

<sup>d</sup>Central temperature calculated from dosimeter data.

<sup>e</sup>Value appears to be low, no explanation for this.

TABLE XIII. Summary of Bend-Test Data on Irradiated U-Mo Alloys<sup>a</sup>

Specimen <sup>b</sup>	Capsule	Specimen History		Burnup Total at. %	Irradiation Temperature °C	Test Temperature °C <sup>e</sup>	Elas. Mod. 10 <sup>10</sup> psi	0.2% Offset Y.S. psi	U.T.S. psi	Strain at Fracture, %
		Fabrication <sup>c</sup>	Heat Treatment <sup>d</sup>							
10 Mo U-1	302-5	1	A	0.06	200	500	8.4		78 000	0.93
10 Mo U-17	9-1	1	B	0.36	500	500 250 25 500	7.6 9.9 10.2 5.9		30 000	0.57
10CT8-4	9.14	2 (Zr clad)	C	0.40	130	500 25 500	5.4 12.2 <sup>f</sup> 5.4	14 600	17 300	0.97
10 Mo U-22	9-2	1	B	0.50	380	500	6.5		25 300	0.39
10 Mo U-13	302-19	1	B	0.91	550	500	7.8		18 700	0.24
10CT4-28	9-14	2 (Zr clad)	C	1.0	200	25 250 500	10.0 <sup>g</sup> 9.6 3.2	17 000	17 100	0.76
11 Mo CE-4	9-11	2 (Zr clad)	C	1.2	400	25 268 25 500	9.7 <sup>g</sup> 7.9 9.5 <sup>g</sup> 4.7	19 900	20 100	0.76
9 Mo Ce-9	9-11	2 (Zr clad)	C	1.2	400	25 250 25	11.1 10.2 10.1			
9 Mo Ce-9	9-11	2 (Zr clad)	C	1.2	400	500	7.9		29 400	0.57
HT-1	9-7	2 (unclad)	D	1.3	470	25	11.7		49 400	0.42
HT-8	9-8	2 (unclad)	E	2.0	600	25 250 25 500	11.7 11.3 14.7 4.0		5 700	0.26
10CT4-25	9-9	2 (Zr clad)	D	2.1	340	25 250 500	5.7 6.6 3.0	11 700	15 700	h

<sup>a</sup>A. A. Bauer, Postirradiation Heating Studies of the Uranium-10 wt % Molybdenum Fuel Alloy, BMI-APDA-646, 3-5-59.  
<sup>b</sup>All specimens are U-10 wt % Mo except 11 Mo CE-4 and 9 Mo CE-9 which contain 11 and 9 wt % Mo, respectively.  
<sup>c</sup>Type of fabrication: (1) Hot rolled to 1/4 in. diam at 900 to 980°C, air cooled, and cold swaged to a 127-mil diam. Irradiation specimens were then machined to 100 mils in diam. (2) Cast billets canned in Zr and co-extruded at 790°C to a 222-mil diam, swaged to 158 mil, and machined.  
<sup>d</sup>Preirradiation heat treatments: A: 24 hr at 900°C and 2 weeks at 500°C, furnace cooled; B: 24 hr at 900°C, water quenched; C: 1 hr at 800°C, water quenched; D: 1 hr at 800°C, water quenched, 1/4 hr at 350°C, air cooled; and E: 24 hr at 900°C, water quenched, 1/4 hr at 350°C, air cooled.  
<sup>e</sup>Test temperature listed in order of performance.  
<sup>f</sup>Average of 3 tests at this temperature.  
<sup>g</sup>Average of 2 tests at this temperature.  
<sup>h</sup>This value could not be computed.

2. No significant differences in the mechanical properties of irradiated specimens fabricated by hot-rolling or coextrusion techniques were observed.
3. The ductility of the reference alloy decreased with increasing amounts of irradiation.
4. The ultimate strength increased slightly with small amounts of irradiation, and then decreased with further irradiation.
5. The modulus of elasticity tended to decrease with increasing burnup.
6. Apparently, at any specified burnup up to 1.0 total at. %, the ultimate strength and the modulus of elasticity of the reference alloy was improved by increasing the irradiation temperature.
7. Zirconium cladding appeared to improve the ductility and strength of the specimens at high burnups.

They noted that the large number of variables and relatively small number of specimens made evaluation of their data difficult. Transformation of the metastable gamma phase at the higher test temperature is known to have occurred during testing. Thus, at the 500°C test temperature, a portion of the changes in the physical properties of the alloy would be due to transformation.

Bauer<sup>13</sup> has reported the dimensional changes that occur when U-10 wt % Mo alloy is heated after having been irradiated. The principal data from his investigation are contained in Tables XIV and XV. Table XIV gives the history of the alloys that yielded the postirradiation data found in Table XV.

Uranium-molybdenum alloys, ranging from 9-13.5 wt % Mo, have been irradiated and reported by Jones et al.<sup>14</sup> Their data give some indication of the effect of molybdenum content on the irradiation stability of U-Mo alloys. Pertinent data on the dimensional stability of these alloys are cited in Tables XVI and XVIII. Exposure data for the specimens in Table XVI are given in Table XVII.

TABLE XIV. History of U-10 wt % Mo Alloys Heated to 430 and 630°C in a Dilatometer\*

Specimen	Cladding and Fabrication Method	Preirradiation Heat Treatment	Irradiation Condition		Postirradiation Changes (%)		
			Temperature °C	Burnup at. %	Density	Diameter	Length
10-PB-4	4 mil, hot rolled pressure bonded	As fabricated at 840°C, furnace cooled	430	1.4	-3.2	0.7	0.6
10-MoU-18	Bare, hot rolled	24 hr at 900°C, water quenched	330	1.8	-3.4	1.0	1.1
HT-2	Co-extruded, declad	1 hr at 800°C, water quenched 17 min at 350°C, ac	600	2.0	-3.5	0.6	1.0

\*A. A. Bauer, Postirradiation Heating Studies of the Uranium-10 wt % Molybdenum Fuel Alloy,  
BMI-APDA-646, March 5, 1959.

TABLE XV. Results of Postirradiation Heating U-10 wt % Mo Alloy Specimens at 650, 700, and 750°C<sup>a</sup>

Specimen	Cladding and Fabrication	Preirradiated Heat Treatment <sup>b</sup>	Irradiation Condition		Postirradiation Changes, %			Post-irradiation Heating		Postirradiation Heating Changes, %		
			Temp. °C	Burnup at. %	Density	Diameter	Length	Time Hr	Temp. °C	Fuel-pin Diameter	Fuel-pin Density	Fuel-alloy Density
10MoTE-33	4 mil Zr, co-extruded	A	500	1.5	- 3.7	0.9	1.4	24	650	1.94	- 7.06	- 7.6
								100	650	7.14	-13.9	-14.9
10PB-5	4 mil Zr, hot rolled, pressure bonded	B	525	1.8	- 3.5	0.9	0.7	24	650	4.3	- 8.55	- 9.4
10CT11-5	11 mil, co-extruded	A	200	1.0	- 1.3	0.58	0.32	4	700	---	- 2.9	- 3.50
								24	700	2.05	- 3.6	- 4.33
								100	700	4.19	- 5.6	- 6.44
10MoTE-30	4 mil, co-extruded	C	245	1.1	- 2.5	0.53	0.63	4	700	---	- 3.5	- 3.75
								24	700	2.49	- 4.6	- 4.95
								100	700	4.34	-----	-----
10PB-4	4 mil, hot rolled, pressure bonded	B	430	1.4	- 3.2	0.7	0.6	4	700	----	- 5.5	- 6.10
								24	700	4.09	- 7.9	- 8.72
10MoTE-40	4 mil, co-extruded	D	245	1.1	- 3.1	1.25	0.84	1/2	750	1.77	- 5.8	- 6.2
								4	750	3.98	- 7.6	- 8.4
								24	750	6.45	-12.1	-13.0
10MoTE-39	4 mil, co-extruded	C	500	1.5	- 3.7	1.2	0.2	1/2	750	1.86	- 4.8	- 5.2
								4	750	3.53	- 7.4	- 8.0
								24	750	6.80	-12.6	-13.5
10MoEC-2	4 mil, co-extruded, swaged end cap	C	400	1.9	- 6.0	1.9	1.3	1/2	750	4.8	-11.9	-12.85
								4	750	9.17	-18.3	-19.8
								24	750	13.90	-26.1	-28.2

<sup>a</sup>A. A. Bauer, Postirradiation Heating Studies of the Uranium-10 wt % Molybdenum Fuel Alloy, BMI-APDA-646, March 5, 1959.

<sup>b</sup>Preirradiation heat treatment: A - 1 hr 800°C water quenched 17 min 350°C, ac; B - As fabricated at 840°C, furnace cooled; C - 1 hr 800°C, slow cool; and D - 1 hr 800°C, water quenched, 2 weeks 500°C, ac.

TABLE XVI. Changes in Dimensions and Density of Transformed U-Mo Alloys<sup>a</sup>

Sample No.	Composition	Heat Treatment <sup>b</sup>	Exposure Mwd/T	Diameter Increase	Density g/cm <sup>3</sup>		Density Change, %
					Preirradiation	Postirradiation	
A 6	U-9 wt % Mo	No. 1	565	n.s. <sup>c</sup>	17.35 ± 0.01	17.34	0
A 8	U-9 wt % Mo	No. 4	755	0.6%	17.47 ± 0.01	17.29	-1.0
A 9	U-9 wt % Mo	No. 4	790	0.7%		17.24	-1.3
B 1	U-10.5 wt % Mo	No. 1	180	n.s.	17.15 ± 0.01	17.16	0
B 12	U-10.5 wt % Mo	No. 4	635	n.s.	17.18 ± 0.01	17.16	---
B 9	U-10.5 wt % Mo	No. 4	730	n.s.		17.11	-0.4

All specimens of U-12 wt % Mo and U-13.5 wt % Mo, having heat treatments No. 1 to No. 4, respectively, showed no change in dimensions or density.

<sup>a</sup>L. J. Jones, M. L. Bleiberg, J. D. Eichenberg, and R. H. Fillnow, Development and Properties of Uranium-Base Alloys Corrosion Resistant in High Temperature Water Part IV, WAPD-127, May, 1957.

<sup>b</sup>Heat treatments: No. 1 - 900°C-24 hr-water quenched; No. 2 - 1 + 525°C-8 hr-water quenched; No. 3 - 1 + 525°C-48 hr-water quenched; and, No. 4 - 1 + 525°C-312 hr-water quenched.

<sup>c</sup>n.s. - indicates no significant change.

TABLE XVII. Exposure Data for Specimens in Table XVI<sup>a</sup>

Sample No.	Composition	Heat Treatment <sup>b</sup>	Internal Thermal Flux (nvt x 10 <sup>-20</sup> )	Exposure Mwd/T	Total Atoms Fissioned, %	Maximum Central Metal Temperature, °C
A 6	U-9 wt % Mo	1	2.09	565	0.066	147
A 8	U-9 wt % Mo	4	2.85	755	0.088	185
A 9	U-9 wt % Mo	4	2.99	790	0.092	192
B 9	U-10.5 wt % Mo	4	2.85	730	0.085	182
B 12	U-10.5 wt % Mo	4	2.46	635	0.074	163
B 1	U-10.5 wt % Mo	1	0.68	180	0.021	74
C 6	U-12 wt % Mo	1	1.02	265	0.031	90
C 8	U-12 wt % Mo	2	2.09	525	0.061	142
C 9	U-12 wt % Mo	2	2.85	700	0.082	178
C 15	U-12 wt % Mo	3	2.99	730	0.085	185
C 16	U-12 wt % Mo	3	2.85	700	0.082	178
C 22	U-12 wt % Mo	4	2.46	610	0.071	160
C 23	U-12 wt % Mo	4	0.68	180	0.021	73
D 2	U-13.5 wt % Mo	1	1.02	260	0.030	88
D 14	U-13.5 wt % Mo	2	2.09	505	0.059	138
D 9	U-13.5 wt % Mo	2	2.85	675	0.079	173
D 15	U-13.5 wt % Mo	3	2.99	700	0.082	180
D 16	U-13.5 wt % Mo	3	2.85	675	0.079	173
D 22	U-13.5 wt % Mo	4	2.46	590	0.069	155
D 24	U-13.5 wt % Mo	4	0.68	170	0.020	72

<sup>a</sup>L. J. Jones, M. L. Bleiberg, J. D. Eichenberg, and R. H. Fillnow, Development and Properties of Uranium-Base Alloys Corrosion Resistant in High Temperature Water Part IV, WAPD-127, May, 1957.

<sup>b</sup>Heat treatments: No. 1 - 900°C-24 hr-water quenched; No. 2 - No. 1 + 525°C-8 hr-water quenched; No. 3 - No. 1 + 525°C-48 hr-water quenched; and, No. 4 - No. 1 + 525°C-312 hr-water quenched.

TABLE XVIII. Changes in Dimensions and Density of Clad U-Mo Alloys (Gamma Quenched)\*

Experiment No.	Composition	Maximum Exposure Mwd/T	Burnup Total at. %	Diameter	Max Calculated Central Temp. °C	Maximum Change	
						Length, %	Apparent Density, %
1 C	U-10.5 wt % Mo	1120	0.13	---	217	n.s.	---
	U-12 wt % Mo	1120	0.13	---	213	n.s.	---
2 C	U-9 wt % Mo	5400	0.65	---	563	n.s.	---
	U-10.5 wt % Mo	5400	0.63	---	555	n.s.	---
	U-12 wt % Mo	5610	0.64	---	562	n.s.	---
	U-13.5 wt % Mo	5610	0.63	---	555	n.s.	---
3 C	U-9 wt % Mo	9980	1.18	---	550	+ 0.24	---
	U-10.5 wt % Mo	9980	1.16	---	542	+ 0.16	---
	U-12 wt % Mo	10 490	1.18	---	552	+ 0.12	---
	U-13.5 wt % Mo	10 490	1.16	---	547	+ 0.08	---
4 C	U-9 wt % Mo	27 800	3.12		647	+ 0.36	- 3.4 (calc.)
	U-10.5 wt % Mo	28 200	3.10		654	+ 0.24	- 3.2 (calc.)
	U-12 wt % Mo	28 200	3.04	+ 2.3	643	+ 0.16	- 3.6 (calc.)
	U-13.5 wt % Mo	28 200	2.99		634	+ 0.16	- 3.4 (calc.)

\*L. J. Jones, M. L. Bleiberg, J. D. Eichenberg, and R. H. Fillnow, Development and Properties of Uranium-Base Alloys Corrosion Resistant in High Temperature Water Part IV, WAPD-127, May, 1957.

Some work has been done by the British<sup>15</sup> on U-14 wt % Mo alloy. Specimens that have been irradiated to a burnup of 0.5 at.% at 800°C have shown a volume increase of 0.5%. Similar work on 9.2 wt % Mo alloy with a burnup of 0.47 at.% at 700°C showed a volume increase of 15%. At 500°C and the same burnup, 9.2 wt % Mo alloy showed a 5% volume increase.

Del Grosso<sup>9</sup> has compiled data on the physical and mechanical properties of the U-10 wt % Mo alloy, the present reference fuel for the Enrico Fermi Reactor. D. O. Leeser et al.<sup>16</sup> have reported results of an investigation of the effect of irradiation on the dimensional stability of U-Mo alloys. A summary of their results, which includes effects of temperature, composition, heat treatment, and cladding thickness, is given in Table XIX. Additionally, they have reported data, shown in Fig. 7, concerning effect of irradiation on the ultimate strength and fracture strain of U-10 wt % Mo at 500°C. Figure 8 presents data on the same alloy that show the effect of irradiation and temperature on the postirradiation elastic modulus, and Fig. 9 contains curves that exhibit the effect of irradiation on the linear thermal expansion of the alloy.

It is difficult to ascertain conclusively the effect of molybdenum on the dimensional stability of these alloys. Referring to the data in Table XVII, which contains data for gamma-quenched alloys, the specimens show a smaller change in length as the molybdenum content increases. However, the density changes recorded do not correspond to this trend. In Table XVI, which gives data for transformed alloys at low burnups, a definite trend of the increase of dimensional stability by molybdenum is noted. A possible explanation for this may be that higher molybdenum alloys contain more of the gamma-prime phase when transformed, and the gamma-prime phase is generally conceded to be more stable dimensionally than the alpha phase when irradiated.

Bauer<sup>17</sup> proposes that an alloy having a composition such that the room-temperature-stable structure would be completely gamma-prime phase may be the best alloy of the U-Mo system for irradiation stability. He bases this proposition on the fact that the gamma phase transforms to the gamma-prime phase by ordering. His theory is that relatively small amounts of irradiation would keep the gamma phase so disordered that it could not transform to the gamma-prime phase, thus yielding a structure that is isotropic in behavior.

TABLE XIX. Summary of Irradiation Results on U-Mo Alloy<sup>a</sup>

Heat Treatment <sup>b</sup>	Alloy Cont.	Irradiation Temp., °C.	Total at. % Burnup	Change, %			
				Density	Diameter	Length	Volume
<u>I. Temperature Effects Series</u>							
B	10	575 ± 25	0.8	- 4.05	2.3	--	--
B	10	575 ± 25	0.8	- 4.40	1.8	0.6	--
B	10	745 ± 25	1.7	-22	15	4.1	--
B	10	745 ± 25	1.7	-24	18	3.5	--
C	10	700 ± 25	0.6	- 2.8	1.1	0.7	--
C	10	700 ± 25	0.6	- 4.09	1.1	0.65	--
C	10	700 ± 25	0.6	- 4.49	2.3	0.75	--
C	10	700 ± 25	0.6	- 5.1	2.5	1.5	--
A	10	630 ± 60	1.3	-23	11.9	8.3	--
E	10	630 ± 60	1.3	-19.8	11.2	6.3	--
F	10	630 ± 60	1.3	-46.8	19.5	5.8	--
<u>II. Composition Series</u>							
A	9	400 ± 60	1.2	- 2.6	1.0	0.4	2.7
A	9	400 ± 60	1.2	- 2.5	0.6	0.5	2.5
A	11	400 ± 60	1.2	- 2.3	0.5	0.4	2.3
A	11	400 ± 60	1.2	- 2.1	1.0	0.6	2.1
<u>III. Heat Treat Series</u>							
D	10	470 ± 70	1.3	- 2.3	0.5	0.6	2.3
D	10	600 ± 90	2.0	- 3.5	0.6	1.0	3.6
A	10	470 ± 70	1.2	- 2.7	0.3	0.5	2.7
A	10	600 ± 90	2.2	- 3.9	0.7	2.3	4.0
B	10	470 ± 70	1.4	- 2.9	0.9	0.7	2.9
B	10	600 ± 90	2.0	- 3.9	1.1	1.0	4.0
<u>IV. Zirconium Cladding Thickness Series</u>							
A-4	10	130 ± 20	0.4	- 1.3	0.2	0.4	0.7
A-8	10	130 ± 20	0.4	- 0.8	0.4	0.3	0.7
A-11	10	130 ± 20	0.8	- 0.5	0.2	0.2	0.5
A-4	10	200 ± 30	1.0	- 1.9	0.8	0.6	2.3
A-8	10	200 ± 30	0.9	- 2.0	0.8	0.4	2.0
A-11	10	200 ± 30	1.0	- 1.3	0.6	0.3	1.5
A-4	10	385 ± 60	2.7	-17.3	9.5	5.1	26.0
A-8	10	385 ± 60	2.1	-15.1	7.9	6.8	24.3
A-11	10	385 ± 60	2.4	- 9.7	5.7	6.9	13.2
A-4	10	340 ± 50	2.1	-15.5	8.3	4.8	22.9
A-8	10	340 ± 50	2.1	- 8.2	3.9	2.1	10.2
A-11	10	340 ± 50	2.0	- 4.2	2.3	0.4	5.1

<sup>a</sup>D. O. Leeser, F. A. Rough, and A. A. Bauer, "Radiation Stability of Fuel Elements for the Enrico Fermi Power Reactor," 2nd International Conference on the Peaceful Uses of Atomic Energy, P/622, 1958.

<sup>b</sup>Number refers to cladding thickness in mils. Letters refer to heat treatments as follows: A: 1 hr 800°C, water quench; B: 24 hr 900°C, water quench; C: 24 hr 900°C, water quench - 2 weeks 475°C, furnace cool; D: as fabricated; E: 1 hr 800°C, slow cool; and, F: 1 hr 800°C, water quench - 2 weeks 500°C, air cool.

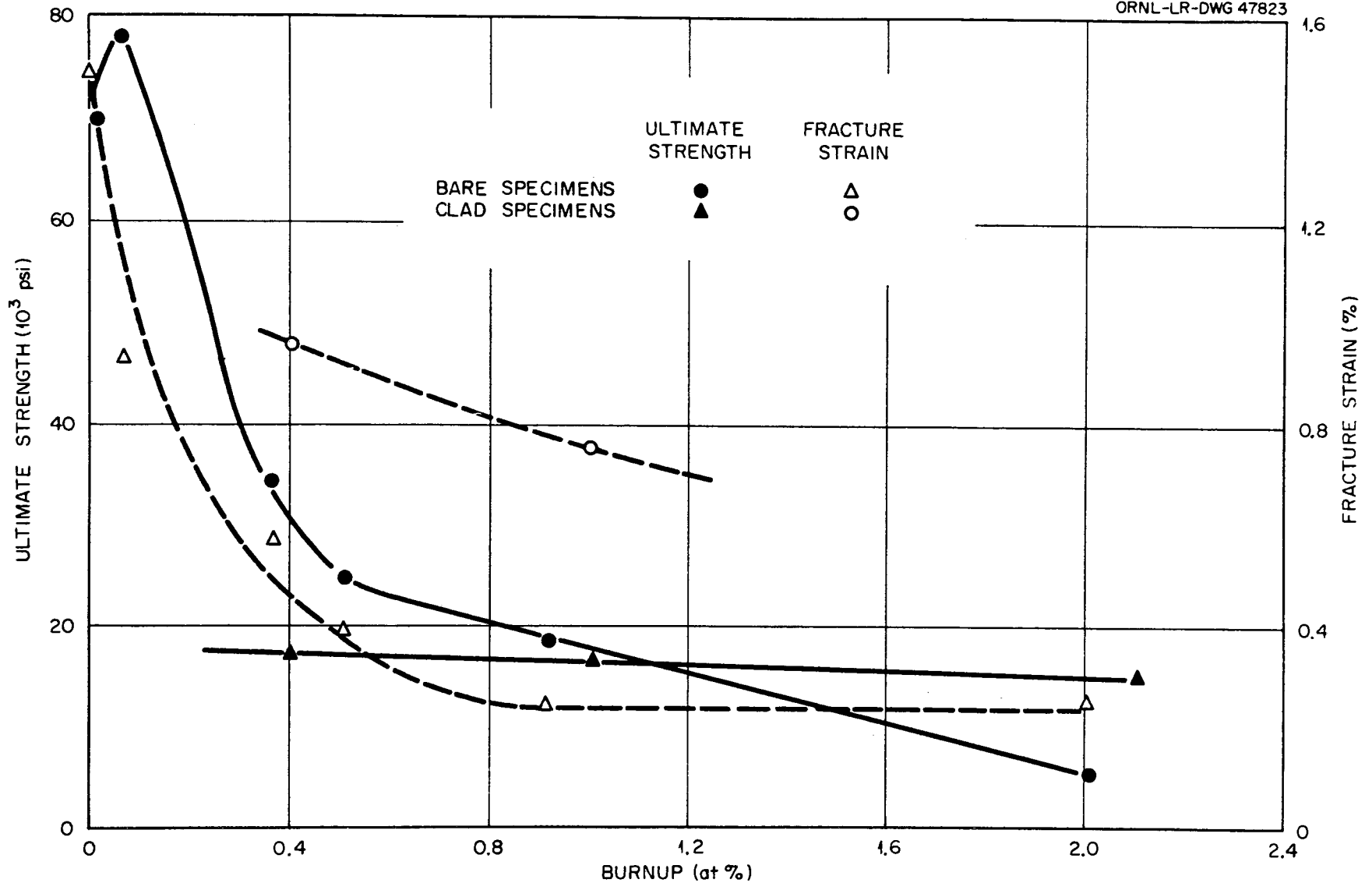


Fig. 7 Effect of Burnup on Postirradiation Ultimate Strength and Fracture Strain of U-10 wt % Mo at 500°C. Reference: D. O. Leeser, F. A. Rough, and A. A. Bauer, "Radiation Stability of Fuel Elements for the Enrico Fermi Power Reactor," Second International Conference on the Peaceful Uses of Atomic Energy, P/622 (1958).

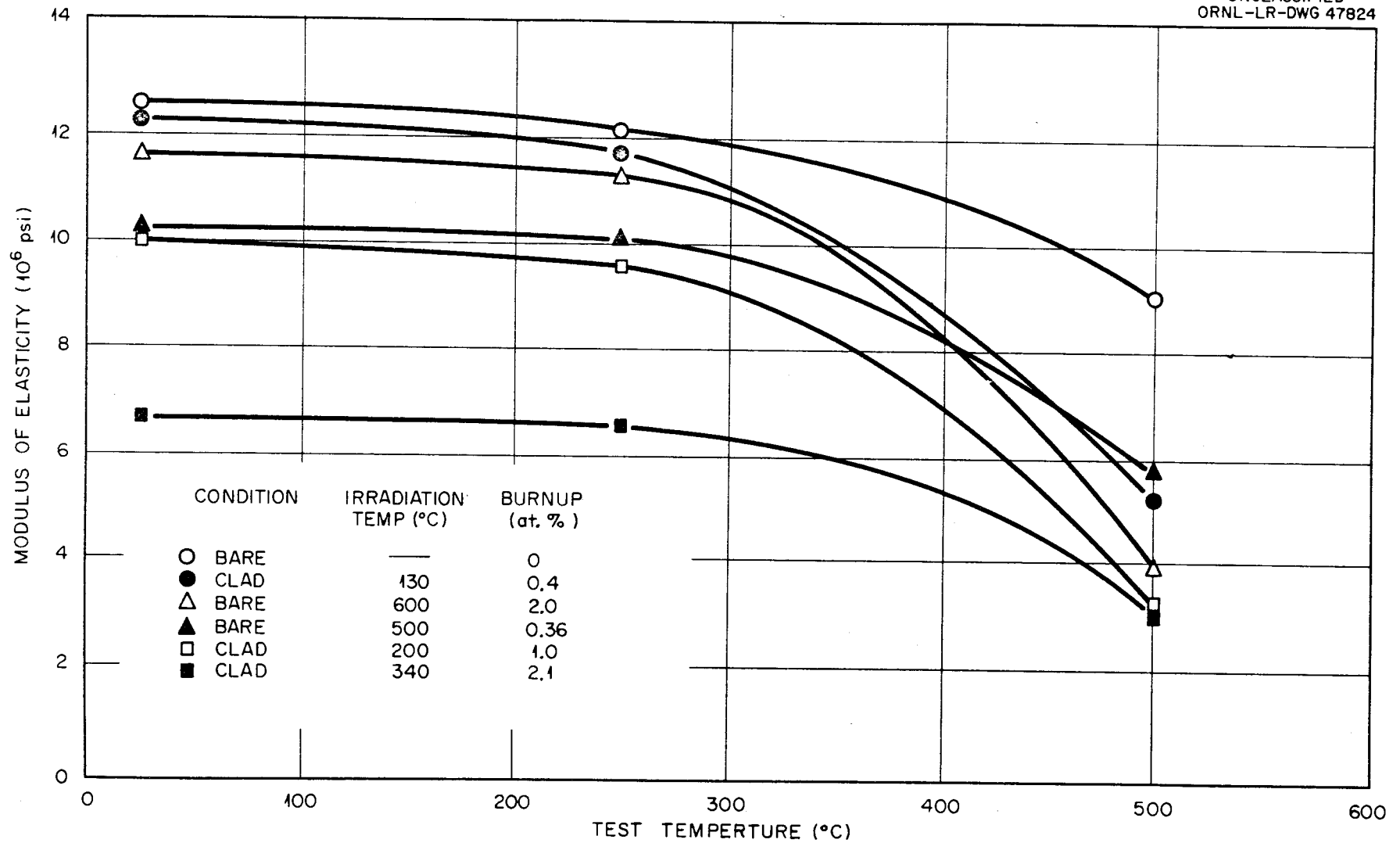


Fig. 8 Effect of Burnup and Temperature on Postirradiation Elastic Modulus of U-10 wt % Mo. Reference: D. O. Leeser, F. A. Rough, and A. A. Bauer, "Radiation Stability of Fuel Elements for the Enrico Fermi Power Reactor," Second International Conference on the Peaceful Uses of Atomic Energy, P/622 (1958).

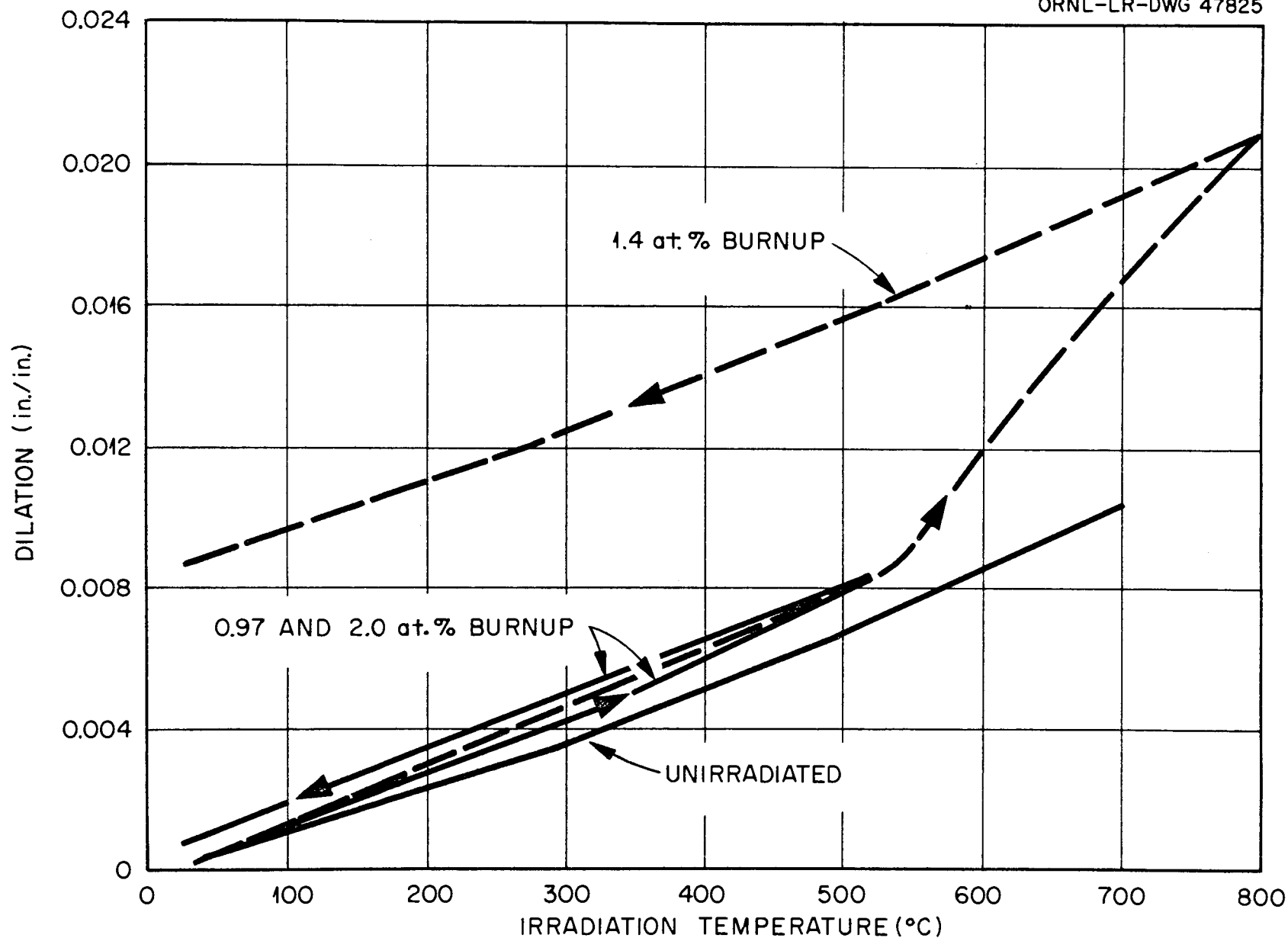


Fig. 9 Effect of Irradiation on Linear Thermal Expansion of U-10 wt % Mo Alloy. Reference: D. O. Leiser, F. A. Rough, and A. A. Bauer, "Radiation Stability of Fuel Elements for the Enrico Fermi Power Reactor," Second International Conference on the Peaceful Uses of Atomic Energy, P/622 (1958).

Several papers<sup>18, 19, 20</sup> claim that in molybdenum-bearing uranium alloys a transformation of room-temperature-stable phases, alpha and gamma-prime ( $U_2Mo$ ), to gamma phase is caused by irradiation at relatively low temperatures (approx 200°C). This phenomenon has been analyzed theoretically<sup>20,21</sup> and shown to be satisfactorily explained by the effect of the thermal spike. A release of considerable energy in a small amount of a substance is an effect of neutron irradiation on fissionable materials. Since the kinetic energy of fission fragments is largely consumed in atomic collisions, the rate of transfer of kinetic energy to the surrounding atoms, at least at the end of the fission-fragment paths, exceeds the rate at which this energy can be removed by thermal conductivity. According to Konobeevsky and his co-workers,<sup>20</sup> an intensive heating of a small region (approx  $10^{-16}$  to  $10^{-17}$  cm<sup>3</sup>) occurs for a time of the order of  $10^{-11}$  sec. In this region the following phenomena may occur: mixing of atoms resulting in disordering and diffusion, recrystallization, disappearance of microstresses or other processes normally occurring at higher temperatures or requiring thermal activation. Brinkman<sup>22</sup> has suggested that this region of intensive heating be called a "displacement spike," retaining the term "thermal spike" for the entire heating path along the trajectory of the primary fast particle.

It has been noted that neutron flux exerts a stabilizing effect on the gamma phase, at least at low temperature. At higher temperatures, however, the thermally activated tendency for gamma to transform may negate the irradiation-induced tendency for stabilization of the gamma phase. Therefore, the gamma phase may indeed transform at such temperatures if the neutron flux is sufficiently low. In irradiations of U-Nb and U-Nb-Zr alloys reported by Thomas *et al.*,<sup>23</sup> the alloys transformed when irradiated at temperatures above 370°C. (The binary uranium alloys contained from 9-12 wt % Nb; the ternary, 10.6 wt % Nb and 4-6 wt % Zr.) Thomas and his co-workers have adopted a model for gamma-phase transformation in which it is postulated that transformation will not occur if displacement spikes occur at a rate sufficiently fast to annihilate nuclei of the new phase before they can grow beyond a critical size, which is one-eighth the volume of a displacement spike. This model gives rise to the

concept of a critical thermal neutron flux, which is the flux below which transformation will occur. The critical neutron flux is given by the following equation:

$$\phi_c = \frac{16 G}{27 N \sigma \alpha v_s} \left( \frac{4 \pi}{3 v_s} \right)^{1/3} \quad (1)$$

where:

- $\phi$  is the critical thermal neutron flux;
- G is the growth rate of the new phase, cm/sec;
- N is the number of  $U^{235}$  atoms per cubic centimeter of alloy;
- $\sigma$  is the microscopic fission cross section of  $U^{235}$ ;
- $\alpha$  is the number of displacement spikes per fission; and
- $v_s$  is the volume of a displacement spike,  $cm^3$ .

The unusually low swelling temperature of some uranium alloys, notably the U-Nb alloys investigated by Thomas, is believed to be associated with transformation of the gamma phase during irradiation. It is apparent to Thomas that fission-gas agglomeration is aided by the sweeping action of phase boundaries and the general low resistance to plastic flow during transformation. He states, therefore, that it is reasonable to believe that improvement of gamma-phase stability has a direct relationship to the swelling characteristics of the fuel alloy. Combining this belief with the model proposed by Thomas, where it is evident that critical flux,  $\phi_c$ , is directly proportional to the growth rate, G, of the new phase, the growth rate of U-Mo alloys should be in accord with their relative transformation rates, some of which are shown in Fig. 3.

A number of means of improving the radiation stability of U-10 wt % Mo alloy have been suggested by Fawcett et al.<sup>12</sup> These are discussed in detail in their report and are as follows:

1. Adjustment of fabrication, homogenization, and heat-treatment process - The alloy is generally homogenized with a heat treatment of 24 hr at 900°C. Material coextruded and heat treated 1 hr at 800°C transforms more rapidly than does hot-rolled material treated 24 hr at 900°C.

2. Quality control of starting materials.
3. Design of subassembly - Flat plate growth expected largely in the direction perpendicular to the plate, may minimize the stress which can cause rupture of zirconium cladding.
4. Alloy additions.
5. Porous alloy fuel.

More importantly, they suggested that  $UO_2$ -U-Mo cermets be considered as a means of increasing the burnup that can be sustained by U-Mo fuels.

### C. Metallurgical Processing of U-Mo Alloys

The general procedure for processing U-Mo alloys includes induction melting and sometimes consumable electrode-arc ~~remelting~~ forging, hot rolling and/or extrusion. Various procedures, which have been used, are subsequently discussed.

#### 1. Melting and Casting

Waldron<sup>2</sup> and his co-workers melted their alloys in a vacuum induction furnace using graphite crucibles, and they cast the alloys in graphite molds. High-purity molybdenum clippings were placed underneath a uranium billet in the crucible. The temperature of the melt was brought to 1500°C and held there for 30 min. During melting, the metal picked up about 0.04% carbon and finished with a carbon content of about 0.07%.

At BMI,<sup>11</sup> the alloys were first induction melted in a vacuum and poured from zirconia crucibles at a temperature of 1590°C into cold graphite molds. These ingots were then melted by the consumable electrode arc-melting process. Additionally, Macherey and Dunsworth<sup>24</sup> at Argonne National Laboratory have melted uranium alloys containing up to 6 wt % Mo by vacuum induction melting technique. They used three types of crucibles: graphite, magnorite, and beryllia. Graphite molds were normally used, but some exploratory castings were made in both thick-walled copper and in steel molds without water cooling in attempts to refine the grain structures by faster cooling. The grain structures of the alloys cast in these chill-molds, however, were about the same as the structure developed in the warm graphite molds.

Foster and Lorenz<sup>25</sup> at the Bettis Plant have investigated the efficiency of various oxide coatings on graphite in producing good quality U-10 wt % Mo alloy. They used a 10-in. diam, internally water-cooled Micarta tube vacuum induction furnace. Melts weighing approx 15 lb were superheated to 1480°C and held at this temperature for 15 min, then lowered to 1400°C for pouring into water-cooled copper molds. Coatings of  $ZrO_2$ ,  $MgZrO_3$ , and BeO on graphite crucibles were used. The  $ZrO_2$ , which was found to be the best coating, was purchased as a slurry from the Titanium Alloy Manufacturing Division of the National Lead Company and was brushed on the crucibles prior to their use. The coatings were approx 0.040 in. thick. The melting crucibles were supported by graphite structural parts, and calcined coke was used as refractory insulation within the vacuum chamber. The stopper rod, for which MgO was the best of the materials investigated, was seated in a hole in the crucible bottom and was mechanically linked to the outside of the chamber. Following induction melting and chill casting to 1-1/4-in. diam, the alloy was remelted to 2-5/16-in. diam by the consumable electrode arc-melting process.

They concluded from the results of their work that:

1. When U-12 wt % Mo was vacuum induction melted in stabilized  $ZrO_2$  coated graphite crucibles, the carbon content increased about 240 ppm and zirconium about 300 ppm.
2. Carbon contamination, but no beryllium contamination was found when BeO-coated graphite crucibles were used.
3. Graphite crucibles coated with  $MgZrO_3$  and high-fired  $ZrO_2$  were found to be unsatisfactory.
4. Consumable arc remelting of the induction melted castings did not improve homogeneity of the material but did result in increased grain size.

Lorenz, Haynes, and Foster<sup>26</sup> report data, shown in Table XX, on the homogeneity and carbon contamination of a typical 50-lb U-12 wt % Mo ingot produced by vacuum induction melting in a zirconia-coated graphite crucible and casting in a graphite mold coated with the zirconia slurry.

Table XX. Homogeneity and Carbon Contamination in a  
Typical U-Mo Alloy Ingot \*

Nominal Composition	Casting Size (in.)	Sample Location In. from bottom	Mo (wt %)	C (ppm)
U-12 wt % Mo	2 diam x 27 long	3.25	11.8	160
		6.50	12.1	170
		9.75	11.9	160
		13.00	12.0	200
		16.25	11.9	160
		19.50	12.0	160
		22.75	12.0	160
		26.00	12.0	170

\* F. R. Lorenz, W. B. Haynes, and E. S. Foster, "Melting and Fabricating Binary Uranium Alloys," J. Metals, 8, 1076-1080 (August 1956).

Lorenz<sup>27</sup> has published a preliminary process specification for melting the U-10 wt % Mo alloy.

## 2. Forging

Forging of uranium alloys containing 10-13.5 wt % Mo could not be done by Waldron<sup>2</sup> and his co-workers, since these alloys tended to crack even at 950°C. They did forge alloys containing 0.85-7.8 wt % Mo at 850°C in air from 2-1/2-in.-diam billets to 7/8-in.-diam rods. In the alpha phase range (about 640°C), all compositions were too hard to forge. The materials oxidized considerably during forging.

Forging at BMI<sup>11</sup> was done at various temperatures depending on the amount of molybdenum contained in the alloy. Both forging and rolling temperatures that they used are given in Table X. Press forging of U-12 wt % Mo has been done by Lorenz<sup>26</sup> and his co-workers at a temperature of about 1950°F (1066°C) using reductions of 1/4 in. per pass. The heating was done in electric resistance furnaces and chloride salt baths. Lorenz states that initial forging should be done cautiously in that the cast structure must first be refined to avoid splitting at the billet ends.

### 3. Rolling

Waldron et al.<sup>2</sup> report that they have rolled 0.85-7.8 wt % Mo alloys in three equal passes at 850°C from 7/8-in. diam to 5/8-in. diam. They were not able to roll 10-13.5 wt % Mo alloys even at 950°C. The BMI<sup>11</sup> rolling temperatures are given in Table X.

### 4. Extrusion

Extrusion of U-10.9 wt % Mo alloys was done by Waldron<sup>2</sup> in a zirconium sheath with a reduction ratio of 16:1 at 850-880°C using a low ram speed of 1/2-1 in./sec. They found that extrusion at normal speeds resulted in transverse cracking.

Uranium-molybdenum alloys have been extruded successfully by Lorenz<sup>26</sup> and his co-workers by heating 2.41- 2.55- and 4-in.-diam billets, varying in length from 3-1/4 to 6-1/2 in., in a chloride salt bath between 1625°F (855°C) and 1775°F (957°C). Their data for 2.41-in.-diam billets extruded from a 2.6-in.-diam container to 0.50-in.-diam rod with a reduction ratio of 27:1 is given in Table XXI.

Table XXI. Extrusion Data of Various U-Mo Alloys\*

Alloy (wt%)	Extrusion Temp. (°F)	Load (tons)		Extrusion Constant(K)psi	
		Start	Finish	Start	Running
U-9 Mo	1775(957°C)	500	350	57 200	40 100
U-9 Mo 0.1 C	1775(957°C)	460	320	56 700	39 400
U-9 Mo 0.5 C	1740(949°C)	510	380	62 900	46 800
U-10.5 Mo	1780(971°C)	450	360	52 000	41 200
U-10.5 Mo 0.1 C	1750(954°C)	375	340	44 800	40 600
U-10.5 Mo 0.5 C	1750(954°C)	450	375	53 800	44 800
U-12 Mo	1750(954°C)	475	390	53 300	43 500
U-12 Mo 0.1 C	1740(949°C)	425	325	50 800	38 900
U-12 Mo 0.5 C	1740(949°C)	375	340	44 800	40 700

\*F. R. Lorenz, W. B. Haynes, and E. S. Foster, "Melting and Fabricating Binary Uranium Alloys," J. Metals, 8, 1076-1080 (August 1956).

They found a mixture of graphite and "Led-Plate" (a lead powder and grease mixture) to be the most satisfactory of the lubricants tried. The best surfaces were produced when using hard-chromium plated steel dies of "Allegheny Ludlum Atlas-A, Hot Die." Hard-faced dies also yielded satisfactory extrusions. All dies used had an approach angle of  $45^\circ$  and a relief angle of approx  $10^\circ$  with a bearing land of  $3/16$ -in. length.

#### 5. Fabrication of U-Mo Fuel Elements

Fabrication processes for producing U-10 wt % Mo fuel elements for the Fermi Reactor have been developed by the Babcock and Wilcox Company and by Nuclear Metals, Inc.<sup>9</sup> Their processes, which are somewhat different, are subsequently described.

Babcock and Wilcox Company (B & W) Process. In the B & W process, the uranium was alloyed and induction-melted under vacuum in a bottom-pour zirconia crucible. The alloy was cast in a zirconia-washed heated graphite mold, yielding a cylinder  $1-5/8$  in. in diameter by 18 in. long. The casting was heated in a salt bath and hot rolled in air at  $1750^\circ\text{F}$  ( $954^\circ\text{C}$ ) to a diameter of 0.90 in. The surface contamination was removed by machining, and the casting was machined to a right cylinder of  $0.810(\pm 0.001)$ -in.-o.d. and cut to  $3.000(\pm 0.005)$ -in. lengths.

A zirconium tube, which had been drawn down to an initial size, was machined to a close tolerance, having final dimensions of  $0.813\begin{matrix} +0.001 \\ -0.000 \end{matrix}$ -in.-i.d., 0.857-in.-o.d., and  $0.022(\pm 0.0005)$ -in.-wall thickness. The tubing was cut to  $3.060(\pm 0.005)$ -in. lengths and deburred.

Standard carbon steel tubing, reamed to 0.875-in.-i.d., was used as a container for the alloy and zirconium tubing for coextrusion. The carbon steel container had an outside diameter of 1 in., a wall thickness of 0.0625 in., and a length of  $3.5 \pm 1/64$  in. Carbon steel nose and tail plugs, used to seal the ends of the coextrusion assembly, were machined from bar stock. To provide a surface for centering the assembled billet in the extrusion die, one side of the nose plug was machined to a point ( $45^\circ$  angle). Thin discs (0.809-in. diam x 0.030-in. thickness), which were used to separate the end plugs from the exposed ends of the billet, were punched from zirconium sheet.

After each component had been cleaned and the carbon steel pieces had been oxidized uniformly to enhance removal after extrusion, the components were assembled; and the end plugs were heliarc-welded to the carbon steel sheath in a helium atmosphere.

The assembled billet was induction heated to 1800°F (982°C) and extruded. The extrusion press utilized a 1.020-in.-i.d. liner, a 0.375-in. die, a 1.182-in.-diam mandrel, and cut-off graphite discs between the ram and extrusion assembly. A reduction of 7.12 to 1, or 86%, was used. The carbon steel sheath was removed from the extruded billet by mechanical stripping and/or by pickling in hot sulphuric acid.

At this point in the process, the clean rod was 0.310 in. in diameter. After the extrusion end defects had been removed from each end of the rod, the rod was cold swaged to final diameter in five passes. Total reduction for the swaging process was 75%, or 3.85 to 1. The swaged piece was sheared, yielding two 30.5-in. fuel elements.

Nuclear Metals, Inc., (NMI) Process. At NMI, uranium was induction-melted under vacuum in a washed graphite crucible and cast in a heated graphite mold, producing a billet 1 in. in diameter and 10 in. in length. The billet was machined to a diameter of  $0.867 \begin{matrix} +0.001 \\ -0.000 \end{matrix}$  in. and cut to lengths of  $2.312 \pm 0.003$  in. An alternate and preferred method, proposed by NMI but apparently not tried, was to cast a 2-in.-diam, 8-in.-long cylinder and reduce it by extrusion to change the as-cast structure before the coextrusion step. If the alternate procedure had been used, a 2-in. liner and a 1.050-in.-diam die would have been employed, providing a 4 to 1 reduction; and a copper can would have been required to prevent oxidation of the uranium.

The machined billet was inserted into a zirconium tube which had been coated on the outside with Alundum ( $Al_2O_3$ ). The tube had an outside diameter of  $0.869 \begin{matrix} +0.001 \\ -0.000 \end{matrix}$  in., an inside diameter of  $0.916 \begin{matrix} +0.000 \\ -0.002 \end{matrix}$  in., and a wall thickness of 0.0235 in., providing a theoretical clad thickness on the finished element of 0.00406 in.

The machined billet in its zirconium sleeve was inserted into an oxidized carbon steel tube having dimensions of  $0.933 \begin{matrix} +0.000 \\ -0.005 \end{matrix}$ -in.-i.d.,  $1.063 \begin{matrix} +0.005 \\ -0.000 \end{matrix}$ -in.-o.d., and 0.065-in.-wall thickness. The outer steel can was required to prevent sticking of the zirconium to the extrusion dies. One end of the tube was spun closed before assembly of the billet, thus forming a pointed end on the extrusion billet.

A Cu-17% Ni preshaped nose piece, the zirconium sleeve, the U-Mo alloy, and a Cu-17% Ni alloy cut-off plug were inserted successively into the steel tube. An evacuation tube was welded to a steel disc, and the evacuation tube assembly was then welded in air to the assembled billet. The assembled billet was evacuated to one micron to prevent oxidation of the uranium and zirconium during the following operations at elevated temperatures. Prior to employment of the Cu-Ni nose piece, a solid steel nose piece had been deemed unsatisfactory because of an excessively high extrusion pressure at the start, which was attributed to the high strength of the steel.

The assembled billet was heated to 1600°F (871°C) and coextruded with an Aquadag lubricant using a 1.10-in.-diam liner and a 0.250-in.-diam die. The extrusion speed was about 60 in./min and the load was 80-85 tons. The large reduction of 18.1 to 1 or 94% was thought to be necessary to provide a good metallurgical bond.

Early extrusions at NMI were unsatisfactory because iron from the steel sheath alloyed with the zirconium cladding. The resultant Fe-Zr alloy could not be removed by wire brushing or pickling without damaging the exterior surface of the clad. After swaging, the Fe-Zr alloy appeared as "stringers" embedded in the zirconium cladding. Additional extrusions were made employing various barriers, such as iron oxide, nickel, chromium, zirconium oxide, Alundum, and various combinations of these materials, to prevent reaction of the steel sheath with the zirconium sleeve. The nickel and chromium barriers were eliminated because small amounts of eutectic were formed. The most satisfactory barrier to eliminate the alloying problem appeared to be an Alundum coating on the outside of the zirconium tube and an iron oxide surface on the steel can.

The steel sheath was removed by pickling in dilute nitric acid, leaving a clean 0.225-in.-diam rod. The extrusion defects, amounting to as much as a 3-in. length from the nose and 12 in. from the rear, were removed.

The extruded rod was then reduced in area 51% by cold swaging using three reductions as follows:

0.225-in. to 0.200-in. diam

0.200-in. to 0.170-in. diam

0.170-in. to 0.158-in. diam

After swaging, the element was ready for cutting into proper lengths, straightening, end capping, and heat treating.

#### D. Powder Metallurgy of U-Mo-UO<sub>2</sub> Fuel Materials

The literature contains information only on the U-Mo-UO<sub>2</sub> investigations carried out by BMI. Apparently, no one else has done significant amounts of work on this system. Two large problems associated with the U-Mo-UO<sub>2</sub> fuel materials are:

1. Obtaining a suitable U-Mo powder.
2. Consolidating U-Mo powder with UO<sub>2</sub> by relatively inexpensive means.

Both of these are subsequently discussed.

##### 1. Processes for Making U-Mo Alloy Powder

Several methods for making U-Mo alloy powder have either been proposed or have undergone some development.

Hydriding. Keller<sup>28</sup> and his co-workers were able to hydride 3.5 wt % Mo alloy slowly in the as-cast condition and quite readily after a water quench from the gamma region. They could not hydride 5- 7- and 10-wt % Mo alloys in either of these two conditions. Attempts were made to hydride 10 wt % Mo alloy in a number of conditions of fabrication and heat treatment and under varying conditions of temperature and hydrogen pressure. They determined two methods by which this alloy can be hydrided: (1) Hydride in an autoclave under 800 psi at 600°C; (2) cold roll the cast product at least 70% to 15-20 mil foil, and hydride the foil under 1-atm pressure and cycle the temperature between 100 and 400°C. The hydride may then be crushed and dehydrided in a vacuum of  $4 \times 10^{-5}$  mm Hg at 360°C. The resulting particle size has been -100 +325 mesh.

Spinning-disc method. Barnes et al.<sup>29</sup> report that they have applied the spinning-disc method to making U-Mo powder. In this method of powder preparation molten metal is dispersed by pouring the molten metal on a high-speed rotating ceramic disc. The method has been used by National Lead Company (NLO) of Ohio to prepare spherical unalloyed uranium powder. Graphite crucibles cannot be used because of carbon contamination of the melt.

The basic spinning-disc equipment consists of a small (3 ft in diameter) vacuum induction-melting furnace adapted to contain a vertically mounted high-speed motor. A 2.5-in.-o.d. steel wheel with a contoured, conical ceramic insert is mounted on the motor shaft. The insert is one inch high and has a diameter along the base of two inches. This wheel is centered in the furnace directly below the pouring lip of a stabilized-zirconium crucible. The alloy charge, consisting of uranium and high-grade molybdenum melting stock, is placed in the crucible and heated to 3000°F (1649°C) under a dynamic vacuum of less than  $2 \times 10^{-3}$  mm of Hg. After alloying is complete, the furnace chamber is backfilled with Bureau of Mines Grade-A helium to an absolute pressure of 1/3 atm; the motor is started; and after the disc speed of 10,000 rpm is reached, the molten alloy is top poured from the crucible onto the spinning disc. The molten material is thrown from the disc, producing a predominantly spherical powder in a range of particle sizes.

The technique resulted from a number of experimental runs in which the characteristics of the system and the alloy behavior were observed and evaluated. For example, the pouring temperature is the mean between two temperature extremes:

1. If the pouring temperature is too low [2500-2700°F (1371-1482°C)], the molten alloy collects on the disc and overloads the motor. In addition, sufficient heat is lost by the alloy to prevent complete removal when poured in a small stream.
2. If the pouring temperature is too high [greater than 3100°F (1704°C)], the metal leaves the disc at too high a temperature, forming irregularly shaped particles or splattering on the furnace walls to remain as a splatter ring.

If molten-metal splash from the disc occurs, the particles tend to be large. By shaping the ceramic disc to a contour which promotes smooth flow of the molten stream, splash is decreased and the powder quality is improved.

Twelve runs were made with 2-kg alloy charges. In two runs no powder was produced. In one run this was due to accidental entrance of air into the vacuum chamber which oxidized the powder product. In the second run this was due to nonconsolidation of off-size powder and disc skulls which had a tenacious oxide film. Further development is required to determine the effect of recycling on the powder quality.

About 60% of the alloy charged to the spinning-disc equipment is converted to powder. Since a significant portion of the 40% loss is the result of splash and the formation of disc skulls, the yield of powder can be increased by increasing the amount of alloy charge. Most of the powder is spherical or near-spherical in shape. Nonspherical shaped particles fall predominantly in the larger particle-size fractions. A sieve analysis of natural U-10 wt % Mo powder prepared by the spinning-disc method appears in Table XXII.

Table XXII. Particle-Size Distribution of Natural U-10 wt % Mo Powder\*

Mesh Size	Average Particle Diameter ( $\mu$ )	Amount in Fraction (wt%)
-12 +18	1350	21.5
-18 +30	800	22.4
-30 +50	410	22.2
-50 +70	250	8.0
-70 +140	150	17.0
-140 +325	75	8.0
-325	44 and under	0.9

\* R. H. Barnes, M. Pobereskin, S. J. Basham, E. L. Foster, Jr., and W. S. Diethorn, Engineering and Nuclear Design Phases of a Paste-Fuel Irradiation Experiment, BMI-APDA-642 (June 4, 1958).

The results of the chemical analysis were as follows:

<u>Impurity</u>	<u>Amount (ppm)</u>
Oxygen	310-380
Carbon	80
Nitrogen	40-50
Hydrogen	7

The oxygen content of the powder is higher than that normally present in cast and wrought alloy. In comparison with uranium-alloy powders prepared by chemical or attrition methods, however, the BMI-prepared powder is lower in oxygen content by a factor of 10.

The as-cast structure reveals the characteristic microsegregation (coring) which occurs even during the rapid solidification in the spinning-disc technique. Battelle Memorial Institute found no visual evidence of transformed gamma phase, and that no transformation occurred was verified by x-ray diffraction studies on the powder. After a 64-hr heat treatment at 500°C in vacuo, the gamma was partially transformed to alpha plus gamma-prime; and after 750 hr at 480°C, it was completely transformed. Battelle Memorial Institute noted that similarity in appearance of the completely transformed and the partially transformed structures is the result of the location and appearance of the predominately gamma-phase makeup of the cored grains. Previous BMI experience, as well as x-ray diffraction, confirms this interpretation of the alloy microstructure.

Ultrasonic and gas methods (atomizing). Additionally, Barnes<sup>29</sup> and his co-workers at BMI tried ultrasonic and gas methods for dispersing molten U-Mo alloys to form powder. In the ultrasonic method, molten alloy is dropped on a transducer head which supplies ultrasonic energy to overcome the surface tension of the molten alloy. The molten alloy then is sprayed out from the transducer head in the form of fine particles, using jets of inert gas for dispersing the molten alloy.

A few experiments with the gas-jet-dispersion method showed that the quality and quantity of the alloy powder were sensitive to jet location. Based on these results, the method was not considered feasible for the production of suitable alloy powder without further development. This method was not further investigated.

Small quantities of nearly spherical powder were produced by the ultrasonic method. The quality and quantity were not satisfactory, however. Powder yields were usually less than 1 wt % of the alloy charged to the device.

Hausner and Mansfield<sup>30</sup> have studied the powdering of uranium by an atomizing process, which may be applicable to making U-Mo powder. In their method, two uranium electrodes were inserted in a dry box filled with argon (99.6% purity) or helium (99.9% purity). One electrode (1 in. in diameter and 6 in. long) was held stationary, and the other uranium electrode (wires varying from 0.09 to 0.25 in. in diameter) was moved by hand. The direction of electrode feed was varied; some runs were made with horizontally arranged electrodes and other runs were made with electrodes arranged in a vertical plane. The power source was a motor generator (dc, 100 amp max). A high-velocity stream of gas (approx 375-400 ft<sup>3</sup>/hr) was sent through a nozzle orifice of approx 1/32 in. in width and about 3/8 in. in length and was directed into the center of the arc. The gas stream covered both the metal vapor in the arc and the molten metal on the face of the electrode.

The characteristics of the uranium powder produced by this method were as follows:

1. Most of the particles obtained by this method approached the spherical shape.
2. The particle size varied between 44 and 2000  $\mu$ , with a predominance of large particles. A typical screen analysis of the powder follows:

<u>Mesh Size</u>	<u>Weight Percent</u>
+10	17.3
-10 +20	55.4
-20 +40	19.5
-40 +60	5.3
-60 +80	1.4
-80 +100	0.4
-100 +140	0.4
-140 +325	0.2
-325	0.1

3. Most of the particles were covered with an oxide film, which was removed by cleaning in nitric acid.
4. The powder was ductile, as shown by hammering the particles to flat thin discs and by compacting in a die.

This powder was deemed unsuitable for powder metallurgy purposes because of the predominantly large particle sizes. Hausner and Mansfield suggested that uranium powder having a small average particle size could be produced in better equipment by proper control of certain variables: notably, current density, rate of feed, and gas flow. Other variables that may need adjustment are voltage, size and shape of electrodes, direction of electrode approach, gas atmosphere, and shape and arrangement of the jet.

Attrition method. No reference to the making of U-Mo powder by attrition has been found in the literature. However, zirconium powder has been made by an attrition method,<sup>31</sup> where chips of zirconium were charged to a "Pulva-mill" that produced predominantly particles of irregular shape. Most of the powder so produced was in the size range of 140 to 200 mesh.

Other methods. Another method considered by Barnes<sup>29</sup> and his co-workers, but rejected, involved the alloying, casting, and fabrication of thin alloy sheet. The sheet would be hydrided, crushed, and sized. After dehydriding the desired fraction, spheres of powder would be produced by dropping the particles through a super-heated vertical tube. This method was rejected because of the expected high impurity of the final product.

## 2. Types of UO<sub>2</sub> for Cermets

Investigators at BMI<sup>32</sup> have worked with spherical UO<sub>2</sub> and have an irradiation program on dispersion fuels well under way. Photomicrographs of their product reveal a distribution superior to the APPR plates. The distribution bears a marked resemblance to the as-hot-rolled product produced early in the APPR development with high-fired oxide, where the fabricated oxide had a characteristic "sweet potato" shape.

The spherical UO<sub>2</sub> made by Mallinckrodt has a porosity of 4.2%, which is higher than the 2.6% porosity for hydrothermal UO<sub>2</sub> as reported by BMI. Keller<sup>32</sup> does not believe the spherical UO<sub>2</sub> to be a high-fired oxide and agrees with Beaver<sup>32</sup> that it is probably similar to Mallinckrodt ceramic grade oxide.

### 3. Uranium-Molybdenum Alloy and UO<sub>2</sub> Powder Consolidation

Keller<sup>28</sup> and his co-workers at Battelle Memorial Institute have fabricated U-Mo-UO<sub>2</sub> cermet by one method in which the U-Mo powder used was produced by the hydriding process and was -100 +325 mesh material. The UO<sub>2</sub> dispersoid was -200 +325 mesh. The U-10 wt % Mo powder (73 wt %) and UO<sub>2</sub> powder (27 wt %) were blended and poured into a type 304 stainless steel tube with a molybdenum barrier between the steel and the loose powder. The tube was then sealed by welding in an inert atmosphere. The tube or can was compacted at 925°C between heated plates with a reduction in thickness of 40%. Following this, the can was annealed 3 hr at 925°C and rolled at 815°C to a 30% reduction in five 0.015-in.-roll passes and water quenched, after which the steel was stripped from the compact.

The U-10 wt % Mo alloy powder does not produce a plate of quality equal to the lower molybdenum-content alloy using the same fabrication procedure. This is attributed to the irregular shaped particles produced by the hydriding operation and to their greater resistance to deformation at 650°C. (The U-10 wt % Mo-containing cermet had to be compacted and rolled at higher temperatures.)

Before the accomplishment of the accomplishment of the above described work, Fawcett et al.<sup>12</sup> had proposed a fabrication procedure to be used for manufacture of zirconium-clad U-Mo-UO<sub>2</sub> cermet fuel elements for APDA. A fabrication flowsheet for this method is shown in Fig. 10.

#### E. Properties of the U-Mo-UO<sub>2</sub> Fuel System

Some irradiation work has been done on the U-Mo-UO<sub>2</sub> fuel material. The specimens, measuring 1 in. x 0.375 in. x 0.040 in., were made using the previously described BMI procedure.<sup>28</sup> Four irradiation specimens were fabricated using a natural U-10 wt % Mo matrix and 27 wt % UO<sub>2</sub> (approx 40 vol %) enriched to 88% U<sup>235</sup>. The densities of these ranged from 13.3 to 13.9 g/cc. The theoretical density of the cermet, based on a density of 17.2 g/cc for the gamma phase U-10 wt % Mo alloy, is 14.85 g/cc. The densities of the specimens are therefore 89.5 to 93.5% of theoretical. Keller et al.<sup>28</sup> and Lesser<sup>33</sup> report the following data on these specimens.

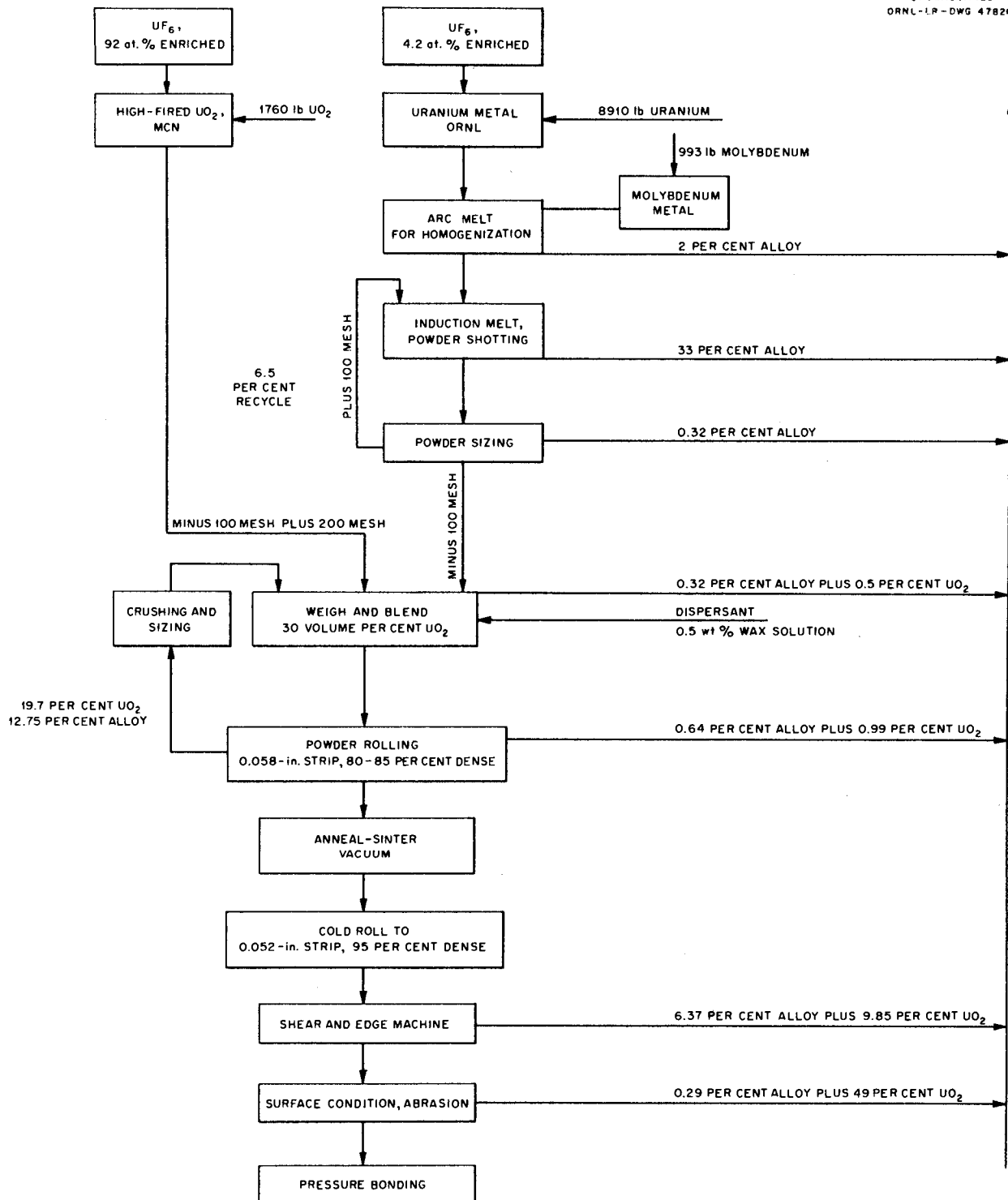


Fig. 10 Fabrication Flowsheet for Flat-Plate 30 vol %  $UO_2$ -U-10 wt % Mo System. Reference: S. L. Fawcett, A Study of Core Fuel Elements for a Fast Breeder Power Reactor, BMI-APDA-636 (Nov. 5, 1957).

### 1. Preirradiation Thermal Cycle Tests

Before irradiation, the specimens were encapsulated in NaK-filled stainless steel cans, the specimens separated from the steel by zirconium baskets, and heated to 700°C. The capsules were thermal cycled by quenching in water from 700°C and then reheating to 700°C. This was done once a day, five days a week. To follow the course of the cycling effects on the specimens, radiographs were taken of the capsules after each cycle. Data from these tests are given in Table XXIII.

### 2. Radiation Tests

Two capsules, each containing two bare specimens, were irradiated in the MTR. The capsules, specifically designed for these irradiations, were neither temperature controlled nor temperature monitored. The burnups and temperatures herein reported were calculated on the basis of dosimeter neutron flux data. The details and results of these tests are given in Table XXIV.

## III. FACTORS INFLUENCING THE DESIGN OF U-MO- $UO_2$ AND OTHER CERMETS

Fundamental studies, based on proposed models, have been made which assist in selecting the types of materials and the type of dispersion which will exhibit maximum resistance to radiation damage. Such factors as particle size of powders, fission product recoil range, and amount of contained dispersoid are basic to the design of cermet fuels. The results of such studies must, however, be used prudently since they are based on models. For example, the model may assume a close-packed arrangement of dispersoid in a matrix, when in actuality the cermet that is fabricated may have the dispersoid distributed randomly.

### A. BMI Design for a U-Mo- $UO_2$ Fuel

In a report to APDA,<sup>12</sup> Fawcett has suggested that they consider a fuel system in which enriched  $UO_2$  is dispersed in a U-10 wt % Mo matrix to obtain high fuel loading and to reduce the amount of radiation damage at high atom burnups. They have compared such a fuel system to others on the basis of energy produced in an equivalent volume of fuel after a designated burnup. A value of unity was assigned to the U-10 wt % Mo alloy after a burnup of 3 at % to provide a comparison. A cermet fuel in which 20 vol %  $UO_2$  is dispersed in a depleted U-Mo matrix will probably withstand irradiation damage to an extent

TABLE XXIII. Results of Preirradiation Thermal Cycle Tests of U-Mo-UO<sub>2</sub> Cermets<sup>a</sup>

Specimen No. <sup>b</sup>	Number Thermal Cycles	DIMENSIONAL CHANGES				Observations
		Percent Changes				
		Weight	Length	Width	Thickness	
1	10	0.06	0.2	0.3	0	All changes within limits of experimental error. The negative change was attributed to chipping of specimen.
2	10	- 0.2 <sup>b</sup>	0.02	0.3	0	
3	39	0.09	0.18	0.37	0	All changes within limits of experimental error except the width change of specimen No. 4.
4	39	0.20	0.25	0.64	0	

CORROSION EFFECTS

Specimen No.	Number Thermal Cycles	Observations
1	10	1. Slight traces of corrosion product on specimens and as solid residue in NaK. 2. Corrosion products were uranium oxide in one phase; another phase contained Cu, Fe, Ni, and Cr, and lesser amounts of U, Zr, and Mn, with slight traces of Mo. 3. Specimens were wetted with NaK more easily after cycling.
2	10	
3	39	
4	39	1. Same as for 1 and 2. 2. Same as for 1 and 2 except there was more uranium oxide and less of the other materials. 3. Same as for 1 and 2.

<sup>a</sup>D. O. Lesser, APDA Memo MAT-242 to A. A. Shoudy Jan. 22, 1959.

<sup>b</sup>U-Mo-UO<sub>2</sub> cermets contained 27 wt % UO<sub>2</sub> (approx 40 vol %) dispersed in U-10 wt % Mo.



comparable to a  $UO_2$ -stainless steel element of 9 at.% burnup of the  $UO_2$  phase. This gives an energy factor of 0.96. By adjusting the enrichment in the matrix so that a burnup of only half that assigned to the reference alloy is obtained in the matrix, the energy factor is increased to 1.3. If the  $UO_2$  loading is increased to 40 vol % and the matrix is depleted, an energy factor of 1.9 is realized if the  $UO_2$  can withstand 9 at.% burnup. Their comparison of the fuel system is shown below.

<u>System</u>	<u>Energy/Equivalent Volume</u>
U-10 wt % Mo (3 at.% burnup)	1
20 vol % $UO_2$ -80 vol % U-10 Mo (9 at.% $UO_2$ burnup, 1.5 at.% U-Mo burnup)	1.3
$UO_2$ (3 at.% burnup)	1.5
20 vol % $UO_2$ -80 vol % U-10 Mo (9 at.% $UO_2$ burnup, 0 at.% U-Mo burnup)	0.96
40 vol % $UO_2$ -60 vol % U-10 Mo (9 at.% $UO_2$ burnup, 0 at.% U-Mo burnup)	1.9

They have also calculated the distance between dispersoid particles as determined by the volume of dispersoid in the cermet and by the dispersoid-particle size, the results of which are shown in Fig. 11. Figure 12 shows BMI results on the volume of nonmetal (oxide plus damaged matrix) that is calculated from various  $UO_2$  loadings and particle sizes when a 6  $\mu$  damage radius is assumed.

#### B. Method for Calculating Irradiation Damage in Cermet Fuels

White, Beard, and Willis<sup>34</sup> have devised a method for calculating damage to cermet fuel materials, which is subsequently described.

##### 1. Conditions for Undamaged Matrix Between Particles

With a close-packing array of spherical particles of uniform diameter, the distance  $d$  between particles is

$$d = \left[ \left( \frac{\pi}{3\sqrt{2}V_f} \right)^{1/3} \right] D,$$

where  $D$  = particle diameter,

$V_f$  = volume fraction of the fuel-bearing phase.

UNCLASSIFIED  
ORNL-LR-DWG 47827

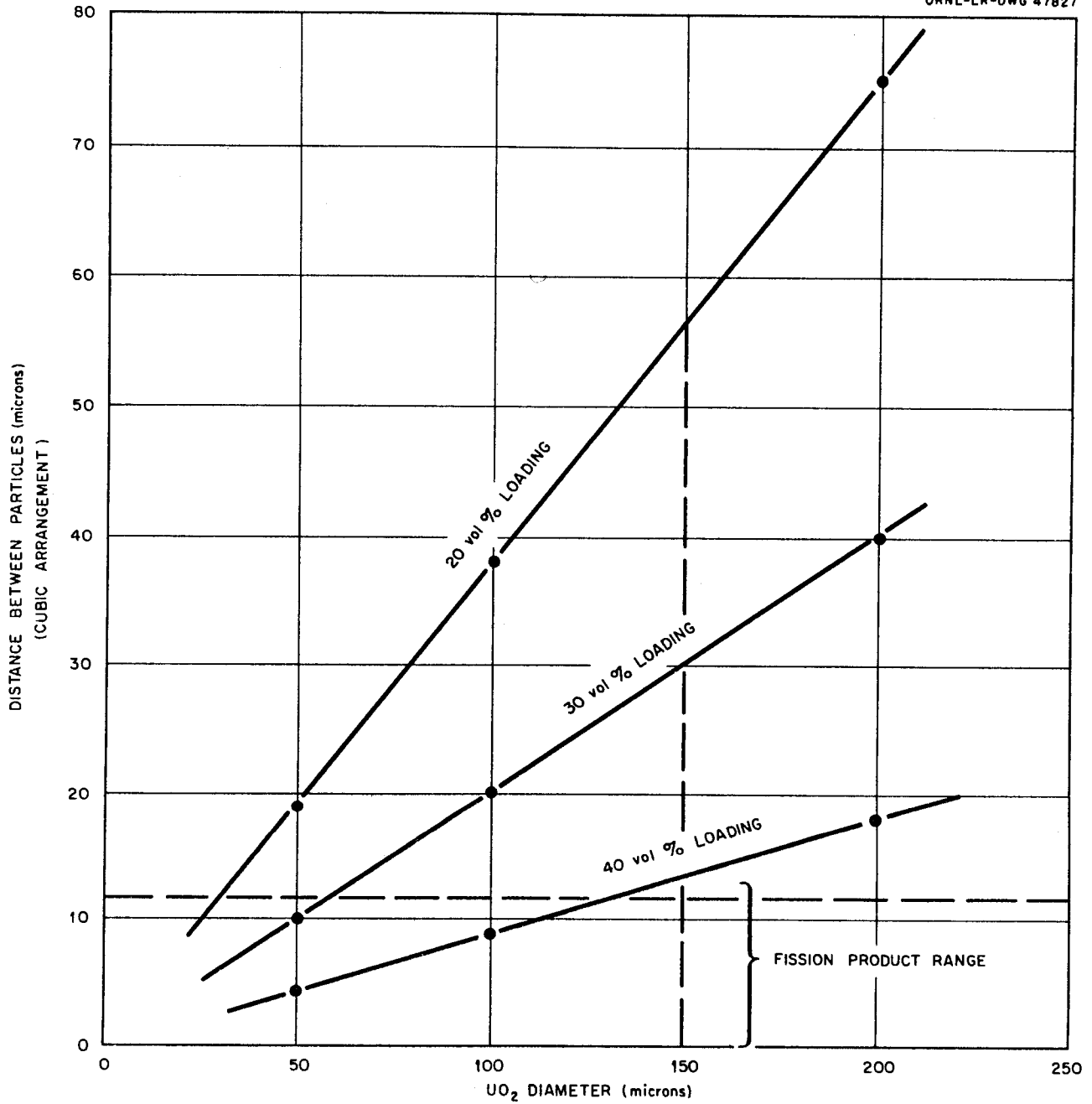


Fig. 11 Relationships Among Oxide Loading, Particle Size, and Minimum Distance Between Particles. Reference: S. L. Fawcett, A Study of Core Fuel Elements for a Fast Breeder Power Reactor, BMI-APDA-636 (Nov. 5, 1957).

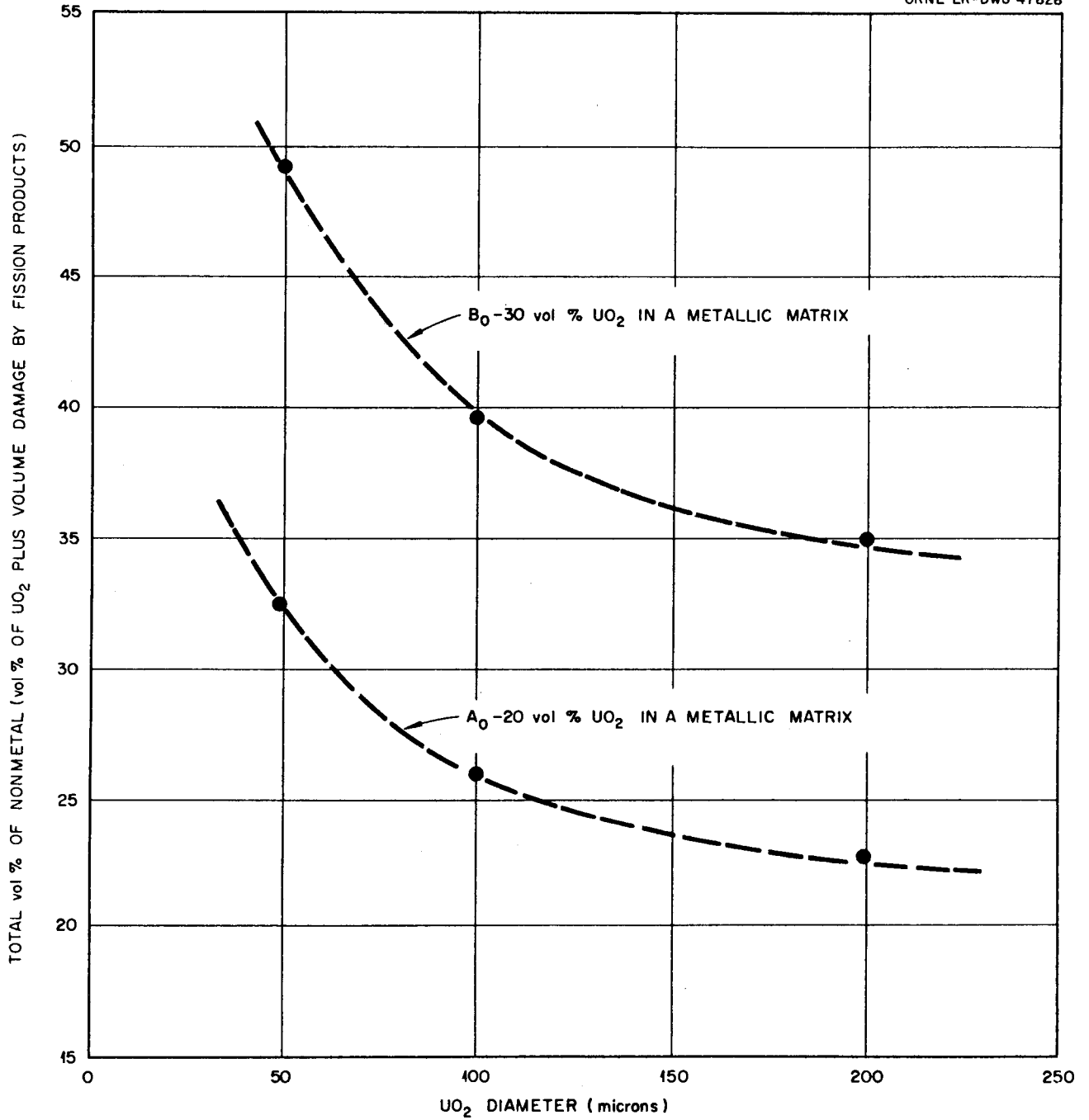


Fig. 12 Effect of Particle Size and Loading on Volume Percent of Oxide Plus Damaged Metal Matrix. Reference: S. L. Fawcett, A Study of Core Fuel Elements for a Fast Breeder Power Reactor, BMI-APDA-636 (Nov. 5, 1957).

Depending upon the size and quantity of the fuel particles and the distance  $\lambda_m$  that the fission fragments penetrate the surrounding matrix, the intervening matrix may or may not be continuously damaged. This is indicated schematically in Fig. 13 and shown graphically in Fig. 14.

$2\lambda_m$  = the thickness of the damaged matrix zones around two adjoining particles.

$d'$  = the thickness of the intervening region free of fission products.

These relationships can be expressed in terms of the ratios  $D/2\lambda_m$  and  $d'/2\lambda_m$ , as follows:

$$D/2\lambda_m = \frac{1 + d'/2\lambda_m}{\left[ \frac{\pi}{(3\sqrt{2V_f})^{1/3}} - 1 \right]}$$

The proportion of damaged matrix to total matrix is given by  $V_{dm}/V_m$

where:  $V_{dm}$  = volume fraction of damaged matrix,

$V_m$  = total matrix in alloy,

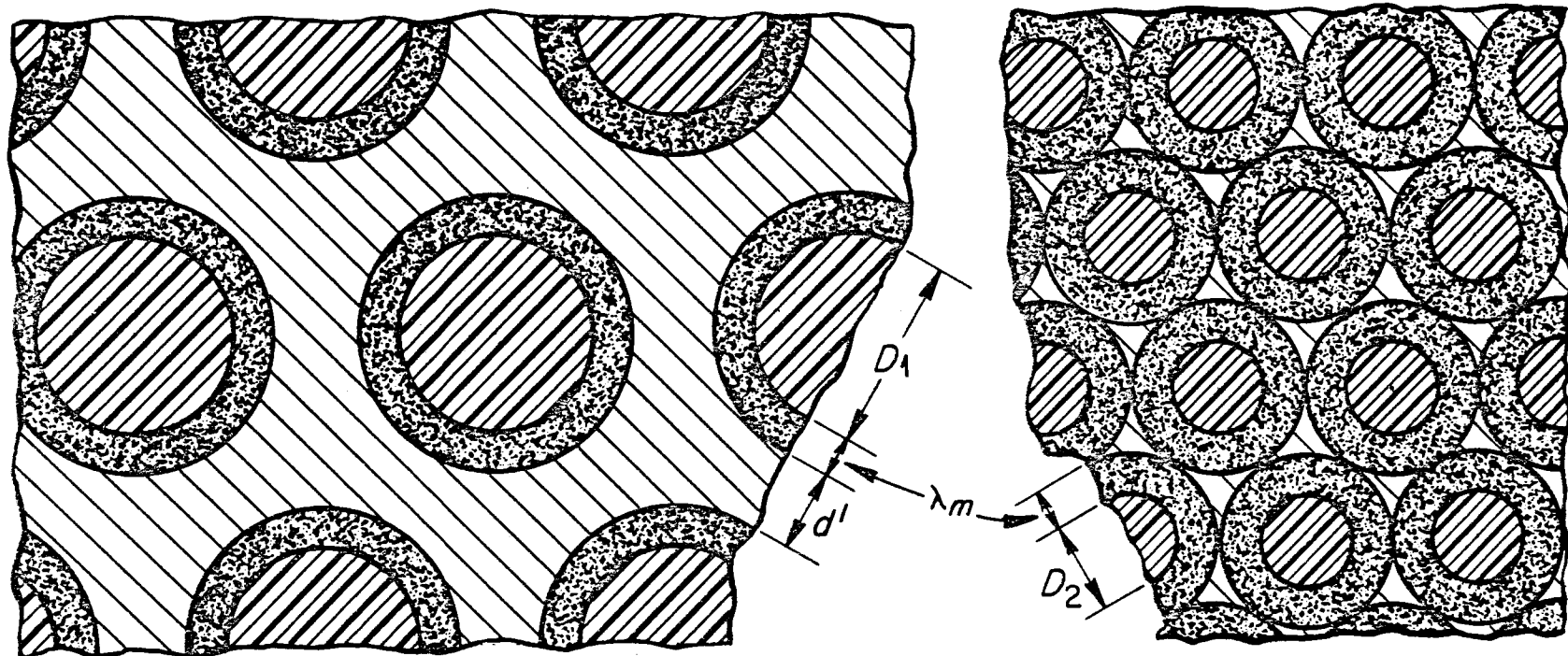
$$\frac{V_{dm}}{V_m} = \frac{V_f}{1 - V_f} \left[ \left( 1 + \frac{1}{D/2\lambda_m} \right)^3 - 1 \right]$$

## 2. Fission Product Content in Matrix

Not only will the alloy properties be affected by the proportion of matrix volume becoming damaged but also by the degree of damage within the affected region. The fraction of fission fragments escaping from each fuel-bearing particle,  $E_{fp}$ , increases as particle size is reduced and as fission fragment recoil range in the fuel phase,  $\lambda_f$ , is increased. The fraction changes are in accordance with the following, as reported by Weber and Hirsch:<sup>35</sup>

$$E_{fp} = 3/4 \left( \frac{2\lambda_f}{D} \right) - 1/16 \left( \frac{2\lambda_f}{D} \right)^3$$

All of the fission fragments escape from the particle when the particle diameter is equal to or smaller than the recoil range. The fuel particles neither gain nor lose atoms when  $E_{fp} = 0.5$ . The dependency of the distribution of fission fragments upon particle diameter is shown schematically in Fig. 15.



FOR CONSTANT VOLUME FRACTION OF PARTICLE PHASE

Fig. 13 Schematic Diagram of the Effect of Particle Size and Spacing on Undamaged Distance Between Particles. Reference: D. W. White, A. P. Beard, and A. H. Willis, Irradiation Behavior of Dispersion Fuels, KAPL-1909, p. 17 (Oct. 1, 1957).

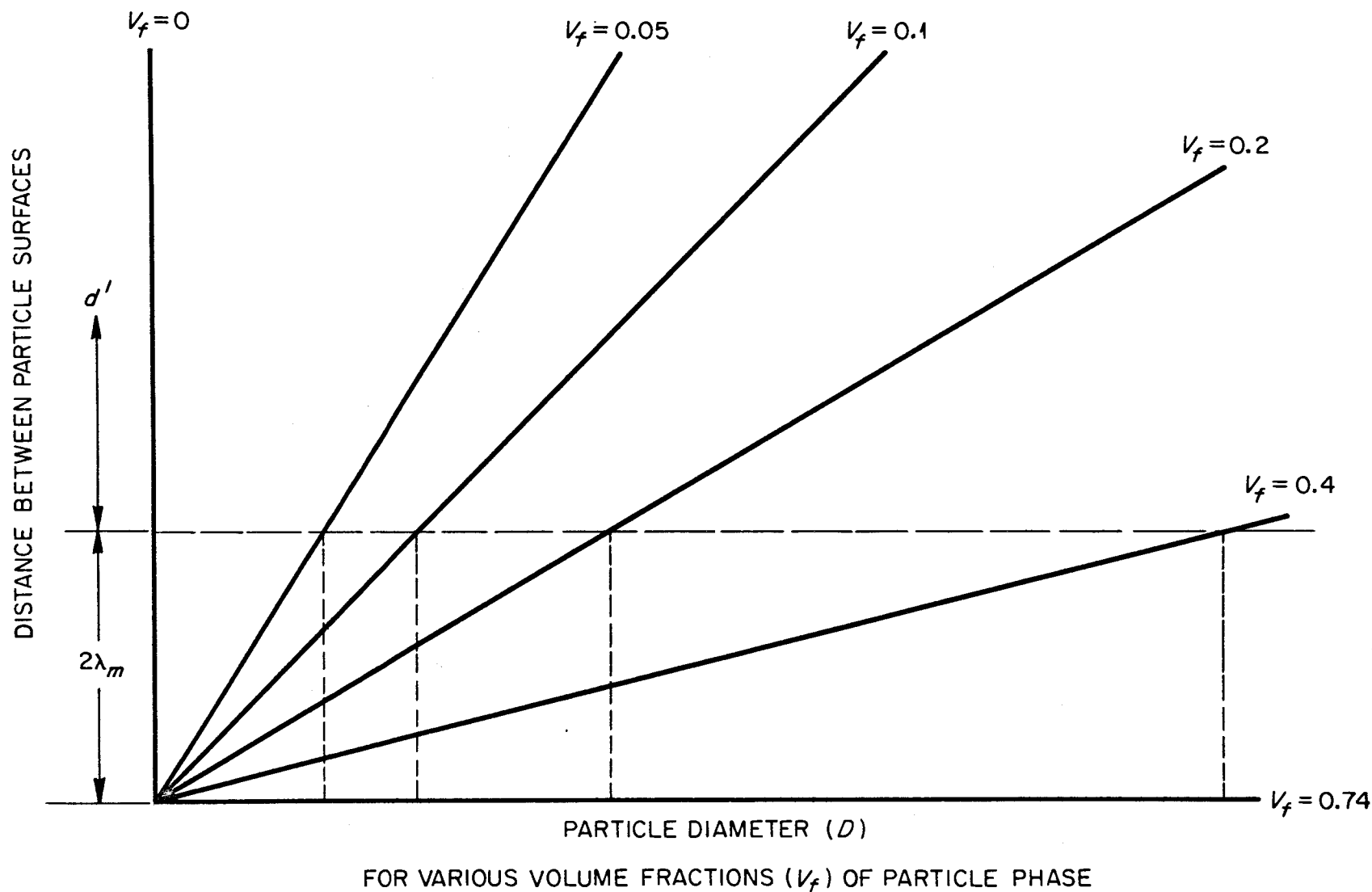


Fig. 14 Effect of Particle Size and Spacing on Undamaged Distance Between Particles. Reference: D. W. White, A. P. Beard, and A. H. Willis, Irradiation Behavior of Dispersion Fuels, KAPL-1909, p. 17 (Oct. 1, 1957).

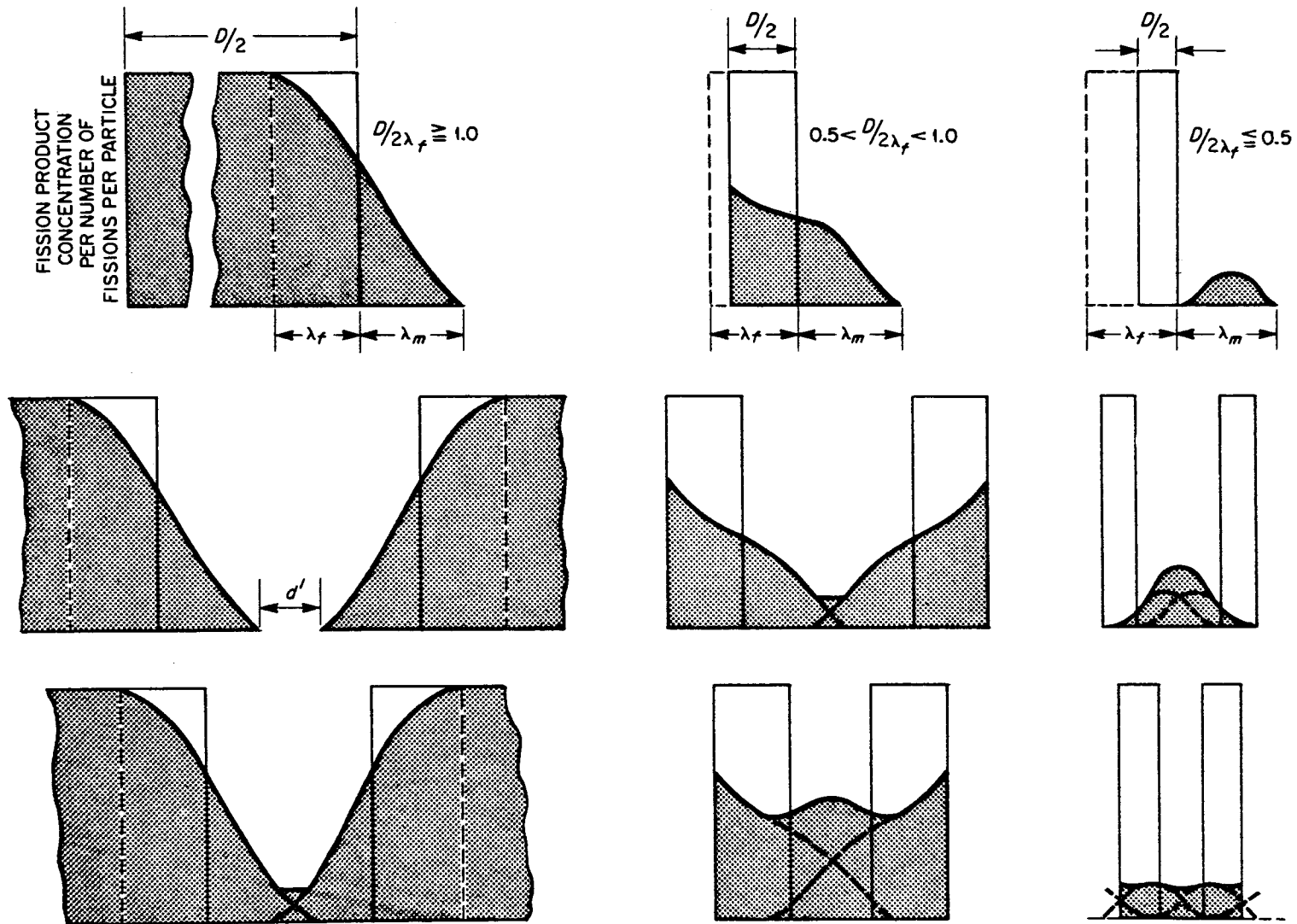


Fig. 15 Distribution of Fission Products in a Matrix. Reference: D. W. White, A. P. Beard, and A. H. Willis, Irradiation Behavior of Dispersion Fuels, KAPL-1909, p. 24 (Oct. 1, 1957).

Various recoil ranges are given in Table XXV.

Table XXV. Fragment Recoil Ranges in Various Materials\*

Material	Average Range ( $\lambda_f$ )					
	For U <sup>235</sup> Fission Fragments			For Particles from B <sup>10</sup> "Fission"		
	mg/cm <sup>2</sup>	$\mu$	in. x 10 <sup>4</sup>	mg/cm <sup>2</sup>	$\mu$	in. x 10 <sup>4</sup>
U	12.6	6.8	2.7	--		
UO <sub>2</sub>	10.0	9.4	3.7	--		
Zr	5.8	9.1	3.6	--		
Fe	5.2	6.7	2.6	--		
Al	3.7	13.7	5.4	1.22	4.8	1.9
Cu	--	--	--	2.0	2.0	0.9
Ag	--	--	--	1.8	1.5	0.6
Pb	--	--	--	2.54	2.0	0.9
B <sup>10</sup>	--	--	--	--	5.1	2.0
SS	--	--	--	--	2.5	1.0

\* D. W. White, A. P. Beard, and A. H. Willis, Irradiation Behavior of Dispersion Fuels, KAPL-1909 (October 1, 1957).

The fission fragments escaping from a particle come entirely from within a thickness of the particle surface,  $\lambda_f$ . The depletion from this zone,  $E'_{fp}$ , decreases with increasing particle size in accordance with:

$$E'_{fp} = \frac{E_{fp}}{1 - \left(1 - \frac{2\lambda_f}{D}\right)^3}$$

The  $E'_{fp}$  values level off at 0.25 for large values of  $D/2\lambda_f$ .

The fission product content per unit volume of damaged matrix,  $M_f$ , is affected by two competing factors. While the number of fission fragments escaping into the matrix (for a given burnup of all atoms in the dispersion alloy)\* increases as the particle size is reduced, the volume of the matrix region in which they become distributed also increases.

\* While  $E_{fp}$  has been defined as the ratio of the number of fission fragments escaping to the number produced per particle, it can be readily shown to be equivalent to the ratio of the total number of fission fragments released to the matrix to the total number produced throughout the alloy.

The net effect is:

$$M_f = \frac{E_{fp}}{\left(1 + \frac{2\lambda M}{D}\right)^3 - 1} .$$

A simplified measure of the net effect on property alteration of the over-all matrix phase may be the average fission product content in the total matrix,  $M'_f$ , which is:

$$M'_f = E_{fp} \left( \frac{V_f}{1 - V_f} \right) .$$

REFERENCES

1. F. A. Rough and A. A. Bauer, Constitution of Uranium and Thorium Alloys, BMI-1300, pp. 41-42 (June 2, 1958).
2. M. B. Waldron, R. C. Burnett, and S. F. Pugh, The Mechanical Properties of Uranium-Molybdenum Alloys, AERE M/R 2554 (1958).
3. E. K. Halteman, "The Crystal Structure of  $U_2Mo$ ," Acta Cryst. 10, 166-169 (March 10, 1957).
4. P. C. L. Pfeil and J. D. Browne, Superlattice Formation in Uranium-Molybdenum Alloys, AERE M/R 1333 (1954).
5. H. A. Saller, F. A. Rough, and D. A. Vaughn, The Constitution Diagram of Uranium-Rich Uranium-Molybdenum Alloys, BMI-72 (June, 1951).
6. R. K. McGeary and W. M. Justusson, Corrosion-Resistant Uranium Alloys, WAPD-227 (Rev.) (June 5, 1953).
7. H. A. Saller, F. A. Rough, and A. A. Bauer, Transformation Kinetics of Uranium-Molybdenum Alloys, BMI-957 (Oct. 21, 1954).
8. R. K. McGeary, W. A. Bostron, M. W. Burkhard, E. K. Halteman, R. D. Leggett, and T. R. Padden, Development and Properties of Uranium-Base Alloys Corrosion Resistant in High Temperature Water - Part I, WAPD-127 (April 25, 1955).
9. A. Del Grosso, Compilation of Uranium-10 w/o Molybdenum Fuels Alloys Properties, AECU-3679 (June 7, 1957).
10. J. E. Gates, E. G. Bodine, J. C. Bell, A. A. Bauer, and G. D. Calkins, Stress-Strain Properties of Irradiated Uranium-10 w/o Molybdenum, BMI-APDA-638 (Jan. 6, 1958).
11. H. A. Saller, R. F. Dickerson, and W. E. Murr, Uranium Alloys for High-Temperature Applications, BMI-1098 (June 25, 1956).
12. S. L. Fawcett, A Study of Core Fuel Systems for a Fast Breeder Power Reactor, BMI-APDA-636 (Nov. 5, 1957).
13. A. A. Bauer, Postirradiation Heating Studies of the Uranium-10 w/o Molybdenum Fuel Alloy, BMI-APDA-646 (March 5, 1959).
14. L. J. Jones, M. L. Bleiberg, J. D. Eichenberg, and R. H. Fillnow, Development and Properties of Uranium-Base Alloys Corrosion Resistant in High Temperature Water - Part IV, WAPD-127 (May, 1957).

15. J. E. Cunningham, Memorandum to R. J. Beaver, Conversation with A. A. Shoudy, APDA, May 5, 1959.
16. D. O. Leeser, F. A. Rough, and A. A. Bauer, "Radiation Stability of Fuel Elements for the Enrico Fermi Power Reactor," Second International Conference on the Peaceful Uses of Atomic Energy, P/622, 1958.
17. A. A. Bauer, Private communication, May, 1959.
18. M. L. Bleiberg, L. J. Jones, and B. Lustman, J. Appl. Phys., 27, 1270 (1956).
19. S. T. Konobeevsky, V. I. Kutaitsev, and N. F. Pravdyuk, "Effect of Irradiation on Structure and Properties of Fissionable Materials," International Conference on the Peaceful Uses of Atomic Energy, P/681, 1955.
20. S. T. Konobeevsky, K. P. Dubrovin, B. M. Levitsky, L. D. Panteleev, and N. F. Pravdyuk, "Some Physico-Chemical Processes Occurring in Fissionable Materials under Irradiation," Second International Conference on the Peaceful Uses of Atomic Energy, P/2192, 1958.
21. S. T. Konobeevsky, Atomnaya Energ. 1, 63 (1956).
22. J. A. Brinkman, J. Appl. Phys. 25, 961 (1954).
23. D. E. Thomas, R. H. Fillnow, K. M. Goldman, J. Hino, R. J. Van Thyne, and F. C. Holtz, and D. J. McPherson, "Properties of Gamma-Phase Alloys of Uranium," Second International Conference on the Peaceful Uses of Atomic Energy, P/1924, 1958.
24. R. E. Macherey and R. J. Dunsworth, The Casting and Fabrication of Binary Alloys of Uranium with Molybdenum, Aluminum, Silicon, Titanium, and Vanadium, ANL-5341 (June 15, 1956).
25. E. S. Foster and F. R. Lorenz, Vacuum Induction Meltings Uranium-12 w/o Molybdenum in Oxide Refractory Coated Graphite Crucibles, WAPD-121 (May 31, 1955).
26. F. R. Lorenz, W. B. Haynes, and E. S. Foster, "Melting and Fabricating Binary Uranium Alloys," J. Metals 8, 1076-1080 (Aug., 1956).
27. F. R. Lorenz, Preliminary Process Specification for Melting Uranium-12 w/o Molybdenum Alloy, WAPD-FE-681 (March 1, 1955).
28. D. L. Keller, D. E. Logier, S. G. Epstein, and A. A. Bauer, Fabrication Development and Irradiation of Uranium-Molybdenum Alloy-UO<sub>2</sub> Dispersions, BMI-APDA-647 (March 12, 1959).

29. R. H. Barnes, M. Pobereskin, S. J. Basham, E. L. Foster, Jr., and W. S. Diethorn, Engineering and Nuclear Design Phases of a Paste-Fuel Irradiation Experiment, BMI-APDA-642 (June 4, 1958).
30. H. H. Hausner and H. Mansfield, Atomization Method of Making Uranium Powder, NYO-1133 (Aug. 7, 1950).
31. A. P. Beard, Private communication, June 10, 1959.
32. R. J. Beaver and D. T. Bourgette, Memorandum to J. E. Cunningham, Visit to BMI, Feb. 19, 1959.
33. D. O. Leeser, APDA Memo MAT-242 to A. A. Shoudy, Jan. 22, 1959.
34. D. W. White, A. P. Beard, and A. H. Willis, Irradiation Behavior of Dispersion Fuels, KAPL-1909 (Oct. 1, 1957).
35. C. E. Weber and H. H. Hirsch, "Dispersion-Type Fuel Elements," International Conference on the Peaceful Uses of Atomic Energy, P/561, 1955.

DISTRIBUTION

- |        |                    |        |                        |
|--------|--------------------|--------|------------------------|
| 1.     | G. M. Adamson, Jr. | 19-23. | A. L. Lotts            |
| 2.     | R. J. Beaver       | 24.    | W. D. Manly            |
| 3.     | E. S. Bomar        | 25.    | M. M. Martin           |
| 4.     | D. T. Bourgette    | 26.    | C. J. McHargue         |
| 5.     | J. A. Burka        | 27.    | P. Patriarca           |
| 6.     | J. H. Cherubini    | 28.    | S. A. Rabinowitz       |
| 7.     | J. E. Cunningham   | 29.    | T. K. Roche            |
| 8.     | D. A. Douglas, Jr. | 30.    | J. M. Robbins          |
| 9.     | J. H. Frye, Jr.    | 31.    | J. L. Scott            |
| 10.    | R. J. Gray         | 32.    | J. D. Sease            |
| 11.    | J. L. Gregg        | 33.    | G. M. Slaughter        |
| 12-13. | J. P. Hammond      | 34-36. | W. C. Thurber          |
| 14.    | W. O. Harms        | 37.    | T. D. Watts            |
| 15.    | T. Hikido          | 38.    | J. R. Weir, Jr.        |
| 16.    | M. R. Hill         | 39.    | H. L. Yakel, Jr.       |
| 17.    | H. Inouye          | 40-44. | A. A. Shoudy, APDA     |
| 18.    | J. T. Lamartine    | 45-49. | Laboratory Records     |
|        |                    | 50.    | Laboratory Records, RC |